

PHOTOCONDUCTION FATIGUE
IN COLORED POTASSIUM CHLORIDE

by

Fred Charles Hardtke, Jr.

A THESIS

submitted to


OREGON STATE COLLEGE

in partial fulfillment of
the requirements for the
degree of

DOCTOR OF PHILOSOPHY


June 1959

APPROVED:




Professor of Chemistry


In Charge of Major



Chairman of Department of Chemistry



Chairman of School Graduate Committee



Dean of Graduate School

Date thesis is presented Sept. 20, 1958

Typed by Lilah N. Potter

ACKNOWLEDGMENT

The author wishes to express his sincere gratitude to Dr. Allen B. Scott for having suggested this problem, and for his continual encouragement and friendly assistance in the preparation of the thesis.

He wishes also to thank all of his colleagues and members of the chemistry department staff who have so generously assisted in this investigation.

The author is greatly indebted to his sister, Clara, for her help in the preparation of the manuscript, and to Lilah Potter and Judy Skow for their assistance in the preparation of the final draft.

TABLE OF CONTENTS

	Page
I. INTRODUCTION	1
Basic Formulations	1
Photoconductivity of Alkali Halides	15
Objectives	27
II. EXPERIMENTAL PROCEDURE	28
Sample Preparation	28
Optical Measurements	33
Photoconductivity Measurements	35
Photoconductivity Cell	39
Thermopile	40
Monochromator	42
Amplifier and Power Supply	44
Motor-driven Switch	48
Polarization Field Measurements	54
III. EXPERIMENTAL RESULTS	55
Photoconduction Fatigue	55
Optical Bleaching	58
Space-Charge Polarization	60
Photocurrent Lag Time	63
Aging	67
Performance of Motor-driven Switch	69
IV. DISCUSSION AND CONCLUSIONS	72
Theoretical Development	72
Symbols Defined	78
Fatigue and Bleaching	80
Interpretation of Results	80
Trap Concentrations and Cross Sections	83
Space Charge Polarization	88
Photocurrent Lag Time	90
PLATES	92
GRAPHS	98
TABLES	110
BIBLIOGRAPHY	114

PHOTOCONDUCTION FATIGUE IN COLORED POTASSIUM CHLORIDE

I. INTRODUCTION

Basic Formulations

Photoconduction or photoconductivity is a term applied to the change in conductivity of a substance upon illumination, and is generally described as an internal photoelectric effect. This phenomenon can be interpreted quite easily. The absorbed photons promote electrons to a conduction level throughout the illuminated volume of the solid material. These photoelectrons leave behind net positive charges, or holes, on the atoms or ions from which they originate. Then the application of an electric field across the illuminated portion of the substance results in the flow of electrons in one direction, holes in the opposite direction; and an electric current, or a photocurrent, is observed. The material is said to be photoconductive.

Even in the absence of an applied field, the electrons and holes continue to migrate within the host material until they recombine or are trapped by impurities or lattice defects. In fact, the presence of an electric field merely introduces a preferential drift in the direction of the field; the average time that the charge

carriers are free to execute their thermal migration remains the same with or without an applied voltage. This average time that a carrier is free is referred to as its lifetime, τ .

For the majority of photoconducting materials the photocurrents are largely, if not entirely, electronic since the holes are relatively immobile. This is certainly true for colored KCl in the wave length region used in these experiments, so that photoconductivity due to holes can be neglected (25, p. 538-539), and only the average lifetime of electrons need be considered. A strictly phenomenological interpretation gives the expression

$$\tau = \left[v (S_h N_h + S_t N_t) \right]^{-1} \quad (1)$$

where τ is the average lifetime of an electron, v the thermal velocity of migration of an electron, S_h the capture cross section of a hole for an electron, S_t the capture cross section of the trapping center for an electron, N_h the concentration of holes, and N_t the concentration of thermally stable trapping centers.

In a single crystal of a pure substance with a perfect crystal lattice the value of N_t may be negligibly small compared to N_h . For this case N_h would equal the

concentration of free electrons, N_e , since for every photoelectron that is formed one hole is simultaneously produced, and when recombination takes place, equal numbers of holes and electrons are obliterated. For practically all photoconducting materials, however, this is a gross oversimplification, since the product $S_t N_t$ is usually comparable to $S_n N_n$ and frequently much larger. Nevertheless, in the limit of a very strong light absorption together with a very high light intensity, N_n will be much larger than N_t even though the latter may be at a considerably high level. As can be seen from equation (1), these stringent conditions yield very small photocurrents due to a greatly reduced \mathcal{Z} , and are, therefore, experimentally avoided. Only the purest forms of germanium and silicon recently manufactured for transistor applications have been found pure enough to satisfy the condition $N_t \ll N_n$ under normal irradiation. When trapping center concentrations are known to be significant, the simple equality between N_e and N_n stated above must be altered to

$$N_e + N'_e = N_n \quad (2)$$

where N'_e is the equilibrium concentration of trapped electrons. Due to the immobility of holes, once an

electron is trapped it will remain in this metastable condition unless thermally released; recombination takes place only between free electrons and holes.

Regarding the thermal stability of trapping centers, three distinct types can be assumed. When a trap is able to hold an electron an indefinite length of time or a time several orders of magnitude longer than τ at the temperature at which the measurements are being conducted, it is considered to be thermally stable. It is only these trapping centers that can be included in N_t of equation (1). A second type is found in those centers that can retain a trapped electron within a few orders of magnitude of τ before it is thermally released. For equilibrium conditions these centers are trapping and releasing electrons at the same rate, so that the steady-state value of τ remains unchanged from what it would be if these traps were absent. However, just as with the first type, they can cause an unbalance between N_d and N_h . Thus, equation (2) is applicable to both types. The third type consists of very shallow trapping centers which act as effective traps for an insignificant length of time compared to τ and are, therefore, treated as though they were nonexistent.

Other phenomenological considerations give two more fundamental relationships

$$N_e = F\tau = I\eta\tau \quad (3)$$

$$\sigma = N_e e \mu \quad (4)$$

which, combined give

$$\sigma = I e \mu \eta \tau \quad (5)$$

where F is the rate of formation of electrons per unit volume, I the rate of quanta absorption per unit volume, η the quantum efficiency,* σ the conductivity, e the unit of electronic charge and μ the field induced electron mobility. Equation (3) is derived from a purely logical argument, while equation (4) is obtained by an application of Ohm's law to a phenomenological description of the electrical current. The combined equation, equation (5), clearly shows that the parameters that characterize a particular photoconductor are η and τ ;

* Quantum efficiency here is defined as the ratio of photoelectrons produced to the number of quanta absorbed. Considerable confusion exists in the literature concerning the two terms quantum efficiency and quantum yield. Normally they could be considered synonymous, as they are in the terminology of the photoelectric effect, color-center conversion, etc. However, in photoconductivity circles an altogether different quantity pertaining to secondary photocurrents has been termed quantum yield. Thus it becomes mandatory that these two terms must be clearly distinguished.

the other quantities appearing in this equation are either easily controlled (I), universally constant (e), or nearly constant for most crystal lattices (μ). This simple dependency on the product $\eta \tau$ constitutes a basic pre-supposition underlying this entire investigation. It is this product which will be frequently referred to as the photoresponse.

It must be emphasized that equation (3) applies only after the attainment of an equilibrium concentration of electrons. Assuming that I , and therefore also F , is constant with time, this is achieved when the rate of recombination, or trapping rate, becomes equal to F . Since at the beginning of the illumination period, the concentration of photoelectrons is zero, the conductivity as given by equation (4) is also zero. The conductivity will continue to rise under prolonged illumination until sufficient time has elapsed whereupon σ takes on its final steady-state value given by equation (5). Then when the illumination is removed, N_e gradually decreases to zero and so does σ . These response times constitute what have been referred to as the rise and decay times, defined as the time that it takes σ to rise or fall to one-half of its final value. In a variety of photoconducting materials this time lag has been observed to vary from 10^{-13} seconds to a few hours (29, p. 1854).

In the event that N_t is much smaller than N_h , the rise time, decay time and τ are all equal. The presence of a significant number of thermally unstable trapping centers greatly extends the rise time to a value well above τ , which is attributed to the relatively slow process of attaining an equilibrium concentration of trapped electrons. Similarly, the slow thermal emptying of filled traps increases the decay time by the same factor.

Stated more precisely, the increased photocurrent response time over the average carrier lifetime, τ , is due to an equilibrium between the number of free electrons and the number of electrons trapped in thermally unstable centers. At any given temperature the number of trapped electrons is directly proportional to the number of conduction electrons. Hence, in order for the photocurrent to decay to one-half of its original value, the number of free electrons, and therefore also the number of shallow-trapped electrons, must be reduced to one-half of their original concentrations. The only way of escape for the trapped electrons is via the free state. Accordingly then, the decay time should be given by the product of τ and $N_t + N_e / N_e$. A similar argument advanced for the rise time would result in an equality between the rise and decay times. This proportionality

between the lag times and τ should be independent of the excitation rate, F , provided only that N_e' is much greater than N_e and that the excitation level is not too high so that some unfilled traps still exist, since then the proportionality factor N_e'/N_e is solely temperature dependent.

Continuing the discussion begun on page 2 concerning the different conditions that prevail when N_t is either negligible compared to N_h or comparable thereto, a means is available whereby these two different concentration levels for N_t can be experimentally discerned. Treating first the case where N_t is much smaller than N_h , equation (1) reduces to

$$\tau = [\nu S_h N_h]^{-1}$$

and, as mentioned on pages 2 and 3, N_e is equal to N_h , so that the above equation can be rewritten as

$$\tau = [\nu S_h N_e]^{-1} \quad (6)$$

Now combining equations (3) and (6)

$$N_e = \left[\frac{n}{\nu S_h} \right]^{1/2} I^{1/2}$$

upon substituting this expression for N_e into equation (4)

it is found that

$$\sigma = e\mu \left[\frac{n}{\nu S_h} \right]^{1/2} I^{1/2} \quad (7a)$$

that is to say, the conductivity is directly proportional to the square root of the absorbed light intensity. For the case where $S_t N_t$ is much larger than $S_h N_h$ equation (1) reduces to

$$\sigma = [\nu S_t N_t]^{-1} \quad (8)$$

Then proceeding as above,

$$\sigma = \frac{e\mu\eta}{\nu S_t N_t} I \quad (7b)$$

the conductivity is found to be directly proportional to the absorbed light intensity.

Thus, an experimental plot of σ vs. $\log I$ should yield a slope of either 0.5 or 1.0 corresponding to the two cases outlined above. Actually, these two extremes are seldom encountered; generally the slope takes on some intermediate value between 0.5 and 1.0. The fact that no slope has ever been observed below 0.5 or above 1.0 offers some experimental verification of the phenomenological treatment employed here, but at the

same time, it becomes clear that neither $S_t N_t$ nor $S_h N_h$ can be neglected in the use of equation (1).*

Thus far no mention has been made concerning the events taking place at the electrodes, yet such effects can profoundly influence the performance of a photoconducting element. Since this investigation involved the measurement only of DC signals, ohmic electrode contacts and blocking contacts must be considered separately. Small barrier potentials permitting the flow of carriers in either direction exist in what have been referred to here as ohmic contacts, while much larger barriers are encountered in "blocking" contacts which, as the name implies, prevent any flow of carriers through the electrode surfaces. A third class, rectifying

* This statement makes no provision for a few materials that have been found to produce a slope greater than unity (30, p. 328-332). This rare behavior has been explained by Rose (29, p. 1859-60) on the basis of the existence of two or more different types of trapping centers of comparable concentrations but quite different cross section ratios for holes and e's. Obviously, the simple form of equation (1) does not apply to these materials. Nevertheless equation (1), as given on page 2, does not exclude the possibility of the presence of different traps; it merely requires that their cross section ratios for holes and electrons be of the same order of magnitude. Since the traps in colored KCl are effective only towards electrons -- the holes being very immobile require no trapping -- equation (1) and the subsequent treatment apply even in the most general case of traps having quite different cross sections for electrons.

contacts, would be either blocking or ohmic for DC measurements.

Ohmic contacts present no special problem. Under sufficiently high electric fields it is possible to have τ exceed the carrier transit time, that is the time that it takes an electron to travel from the anode to the cathode. The photocurrent observed will then exceed the ratio of formation of electrons (I_n) by a factor τ/T_n where T_n is the carrier transit time. The ratio τ/T_n has been termed the quantum yield. Photocurrents having a quantum yield greater than unity puzzled early investigators who quite erroneously labeled such currents as secondary photocurrents, believing that an altogether different mechanism was responsible for their occurrence.

Secondary photocurrents, that is currents that actually do arise independent of the mechanism formulated above, have been observed when blocking electrodes are employed. When a primary photocurrent is drawn from a photoconducting element equipped with such electrodes, a charge separation occurs which results in the build-up of electrical double layers near the electrode surfaces, thereby giving rise to an internal electric field opposed to the external applied field, and a marked decrease in the photocurrent results. This decrease in photocurrent should follow an exponential decay with time provided

that the entire volume of the photoconducting element is uniformly illuminated and that the separated charge is completely contained in thin surface layers. However, due to the very high electric fields developed at the electrode surfaces by the double layer formation, field emission can, and does, occur producing a truly secondary current. Secondary currents caused by bombardment induced charge carrier multiplication, analogous to that occurring in a discharge tube, have not been observed in photoconductivity measurements undoubtedly because of the short range of photoelectrons.

As mentioned previously these secondary effects can be avoided through the use of ohmic contacts. Unfortunately, no such electrode materials have been developed for the alkali halides. Hence, in working with these materials, an experimental means must be provided to minimize the effect of space-charge build-up which reduces the desired primary photocurrent and simultaneously introduces spurious secondary currents.

Since the conductivity as given by equation (5) is independent of the opposed electric field, a direct proportionality between the photocurrent and field strength is to be expected. Experimental confirmation has been obtained for ohmic contacts, but not completely for photoconducting materials equipped with blocking

electrodes. For the latter, a proportionality usually exists at low applied voltages. However, as the field increases, the photocurrent frequently approaches a saturation value. A plausible explanation is found when one considers the average carrier drift in the direction of the applied field, or shubweg, in relation to the dimensions of the photoconducting specimen. The shubweg, d , can be expressed in terms of previously defined quantities as

$$d = \mu E \tau \quad (9)$$

When E is increased, beginning with a low voltage, a proportional increase in d occurs until d becomes comparable to the specimen dimension parallel to the direction of the field. At this point the photocurrent approaches the rate of formation of photoelectrons, F . A further increase in voltage will not result in an increased photocurrent since the blocking electrodes prevent any electrons from entering or leaving the photoconductor. Whether or not a saturation in the photocurrent is observed depends to a large extent on the value of τ in equation (9). For materials having a very short τ , sufficiently high electric fields to produce saturation may not be experimentally obtainable.

This saturation phenomena, if it can be achieved experimentally, permits an evaluation of the quantum efficiency, η . Since the photocurrent, i , is equal to VF or $VI\eta$, after saturation has been attained, then

$$\eta = \frac{i}{VI} \quad (10)$$

where i , I , and V , the illuminated volume, are experimentally determined quantities. Of course, it is to be assumed that the problem of secondary currents accompanying the use of blocking electrodes has been experimentally circumvented.

Much of the above treatment was based on two review articles given by Rose (29, p. 1850-1869 and 28, p. 362-413). Other reviews on the general topic of photoconductivity can be found in Mott and Gurney (17, p. 117-140), Petritz (20, p. 49-77), and Hughes and du Bridge (8, p. 284-351). A rather complete mathematical presentation of space charge effects occurring with blocking electrodes is given by von Hippel, et al (38, p. 568-574).

Photoconductivity of Alkali Halides

Pure uncolored alkali halides exhibit no measurable photoconductivity throughout the ultraviolet, visible, and infrared wave length regions. This includes the fundamental absorption band in the ultraviolet, where a number of ionic insulators are quite strongly photoconducting. Beyond the fundamental absorption band, and continuing on out to the far infrared region, the alkali halides are completely transparent, so that a photoresponse would not be expected in this entire wavelength region. To what extent the lack of photoresponse in the region of fundamental absorption is due to a very low or to a greatly reduced τ has not been resolved at the present time (17, p. 104). Regardless of the role that η plays in this process, the greatly reduced τ , caused by a very rapid electron-hole recombination rate in surface layers where ultraviolet light is strongly absorbed, would certainly be expected to limit the photoresponse to some very small value.

On the other hand, when alkali halide crystals are colored by any of the method commonly employed, they become quite photoconducting in the fundamental absorption band (9, p. 898) and also in the newly formed absorption peaks introduced by the coloring process.

Nearly all of the absorption bands that have been investigated display maximum photoresponses with monochromatic illumination having wave lengths coinciding with the peaks in the optical absorption spectra. For example, the peak of the so-called F-band occurs at $560\text{ m}\mu$ for KCl, and the wavelength producing a maximum photoresponse in KCl crystals containing the F-band is also $560\text{ m}\mu$. As an exception to the general statement, the maximum photoresponse of a broad band, now identified as the colloidal band, is shifted well to the ultraviolet side of the corresponding absorption band. Gyulai (5, p. 413-414), and later Nielsen and Scott (18, p. 302-303), have attributed this shift to a photoelectric effect involving colloidal particles of alkali metal. One other exception is found in the unusually flat photoresponse observed in, or near, the fundamental absorption band. This has been interpreted recently by Inchauspe (9, p. 898) on the basis of an exciton mechanism for the liberation of photoelectrons from F-centers. Aside from these exceptions just mentioned, and neglecting any comparison of peak heights, the spectral distribution of photoresponse follows very closely the optical absorption spectra for all of the colored alkali halides. From this, it can be concluded that charge carriers, presumably electrons, are produced by the absorbed quanta

and that the same photoncolor center interaction responsible for the absorption band is likewise responsible for the photoconductivity.

The topic of photoconductivity in colored alkali halides has been reviewed by Pohl (23, p. 15-20), Mott and Gurney (17, p. 117-137), Hughes and du Bridge (8, p. 284-321), and most recently by Seitz (32, p. 563-571 and 33, p. 44-46, 75).

Of the numerous absorption bands that have been detected in colored alkali halides none of them shares the prominent position which is occupied by the F-band. Some of the reasons for the prominence it has achieved are: (1) Historically it was the first color band to have been studied in any great detail. This work was done by Pohl and his associates, who pioneered much of the work on color centers in alkali halides. The "F" in the terms "F-band" and "F-center", derived from the German Fahbrenzentren, stands as a monument to their important contribution. (2) The present day model of the F-center, originally proposed by de Boer, has withstood nearly 30 years of experimental and theoretical scrutiny, although there is still no direct experimental proof of the model, while the exact nature of the several other bands is still somewhat uncertain. (3) It is the only absorption band which can

be successfully produced in the absence of other absorption bands. This can be accomplished in the initial coloring process through the careful exclusion of light and a suitable control of the temperature.

The first photoconductive measurements of colored alkali halides appear to have been carried out by Rontgen (27, p. 116-195). Soon thereafter, Glaser and Lehfeldt (23, p. 18) conducted some exhaustive experiments in which they determined the temperature dependency of the F-band photoresponse, and established the existence of a second color band located on the long wavelength side of the F-band. They named this band the F'-band because of its close relationship to the F-band.

Regarding the temperature dependency, it was found that beginning with very low temperatures the photoresponse, η^{τ} , was negligibly small until a temperature (-180° C for KCl) was reached whereupon a sharp rise in η^{τ} with temperature was observed. Following this sharp rise, the photoresponse remains nearly constant with further increases in temperature until a second rise occurs (at -75° C for KCl), which likewise levels off to a constant value towards further increases in temperature. In the region of the first plateau in the above plot of η^{τ} vs. temperature (-140° to -75° C for KCl) the F'-band

is found to grow in size while the F-band diminishes during prolonged illumination in the F-band. Furthermore, Pick (22, p. 371-374) had observed that the quantum efficiency for the destruction of F-centers has a value very close to 2.0. That is, for every quantum absorbed in the F-band two F-centers are destroyed. Also in this same region of the ϕ vs. temperature curve, the photoresponse is found to be inversely proportional to the F-center concentration within the range of 5×10^{15} to 1×10^{18} F-centers per cubic centimeter. Then in the region of the second thermal rise of the photoresponse, a very appreciable lag time of the order of a few seconds was observed, while elsewhere on the curve no measureable lag time was ever detected.

Beginning with the well established model of the F-center consisting of an electron trapped in the potential field of a halide ion vacancy, the above findings of Glaser and Lehfeldt can be quite easily explained. Tibbs and Simpson (35, p. 1478-1484 and 34, p. 278-280) have calculated the energy levels to be expected for an electron moving in the potential field of the ions surrounding a halide ion vacancy in NaCl. Although their calculations require some refinement to obtain a better agreement with experiment, qualitatively at least, the photoresponse in the region of low

temperature can be interpreted from their results. Tibbs found two energy levels separated by 2.4 ev with the excited state 0.6 ev below the conduction band. The corresponding experimental values are 2.7 ev and 0.1 ev, respectively. Raising an electron from the ground state to the excited state corresponds to the photon absorption process producing the F-band. While in this excited state, before it returns to the ground state, the electron must be thermally released in order to become a photoelectron. This explains why no photoresponse is obtained at very low temperatures. In simple qualitative terms, the quantum efficiency is zero until a sufficiently high temperature is reached to release electrons that are raised to the excited state. A quantitative explanation given by Mott and Gurney (17, p. 135-136) for the increase of η with temperature fits the first thermal rise in photoresponse quite well. Thus, this initial thermal increase in $\eta \tau$ is attributed entirely to an increase in η , whereas the second thermal rise must be accredited to an increase in τ , since η attains a maximum value, presumably unity, during the first thermal rise.

Ample evidence exists for this interpretation of the second thermal rise in photoresponse. Consideration of equation (1) shows that the inverse proportionality

between the photoresponse and the F-center concentration identifies the effective trapping centers below the second thermal rise as F-centers themselves. This conclusion is further substantiated by the observed value of 2 for the quantum efficiency of F-center destruction, for when an F-center traps a free electron two F-centers are destroyed -- the one from which the electron originated, and the one which has trapped the photoelectron. Thus, the F' -center is to be identified as an F-center which has added a second electron. Returning to the problem of explaining the second thermal rise, it can be seen from the discussion given on page 7 that the appearance of a photocurrent lag shows that the increase in photoresponse can be attributed to an increased χ due to the F' -centers becoming thermally unstable. This interpretation is in agreement with the fact that the F' -band is not found above this temperature region.

The first study of photoconduction fatigue in the F-band appears to have been made by Oberly (19, p. 1257-1258), who found a marked decrease in photoresponse in both the F and M-band regions accompanying the optical bleaching of the F-band. The per cent decrease in photoresponse in the F-band greatly exceeded that of the optical absorbancy. In addition, Oberly reported that

the rate of weakening of both the optical absorbancy and the photoresponse decreased with increasing time of exposure. On the basis of these findings he attributed the fatigue in photoresponse, $\eta \tau$, to a decrease in η rather than τ , and supported his findings with evidence that any decrease in $\eta \tau$ due to a changing τ is not readily understandable. To account for the decrease in η , he suggested that two types of F-centers may exist: a soft center which is photoconducting and also readily bleached by light ($\eta = 1$), and a hard F-center which is not photoconducting and is relatively unaffected by light ($\eta = 0$).

The supposition that the F-band is in reality two or more bands superimposed in each other is not new. Earlier Oberly and Burstein (1, p. 217) noted that the quite different photoresponse of the F-band in the presence of the R, M and N-bands on the one hand, and in the absence of these same bands, on the other hand, could be interpreted using such a model of the F-band. Much earlier Przibram (24, p. 406-407) had uncovered evidence for the existence of two different types of F-centers. The work of Petroff (21, p. 449-450) on the rate of conversion of F-centers to M-centers in KCl also has a bearing upon this subject. He reported that the transformation apparently takes place by means of an

intermediate stage which has an absorption peak corresponding to the F-band. The measurements of the dichroism of the F and M-bands recently performed by van Doorn and Haven (37, p. 753) add weight to this supposition. Markham, et al. (14, p. 600) found that the X-rayed colored alkali halides can be partially bleached even at very low temperatures (5° and 78° K) and described their findings in terms of "hard" and "soft" F-centers. Markham (15, p. 770-771) clarified his viewpoint by proposing that all F-centers are fundamentally identical, only differences in their environment of vacancies and V-centers are responsible for the apparent "hard" and "soft" properties. Since this low temperature bleaching was not observed in crystals colored by heating in the presence of alkali metal vapor (additive coloration), it was concluded that crystals colored in this manner have more nearly perfect crystallinity. Finally, very recently Konitzer and Markham (10, p. 685-686) reported a very slight broadening of the F-band under various bleaching treatments and attributed this to the existence of a second band under the F-band in agreement with the findings of Petroff (21, p. 451-453).

The assumption of "hard" and "soft" F-centers leads to certain difficulties, however, when a comparison

is made of the quantum efficiency observed by others with the quantum efficiency predicted by this model of the F-band. It can be seen that the value of η would never exceed the ratio of the concentration of "soft" centers to the total concentration of centers. Thus, for any appreciable concentration of "hard" centers, a value significantly smaller than unity would be expected for η . This is contrary to the well established findings of Glaser and Lehfeldt and Pick already referred to on pages 18 and 19, where a quantum efficiency approximating unity was observed. Unfortunately, a direct measurement of η by the field-current saturation technique described on page 13 has not been successfully accomplished for alkali halides. At about 40,000 volts per centimeter Flechsig (3, p. 790) obtained a saturation current using very thin crystals -- too thin for satisfactory measurement of the light absorption. More recent attempts do not appear to have been made.

Markham (16, p. 433) suggested that the decrease in the product $\eta\tau$ which Oberly observed during the bleaching of the F-band could be due to a decrease in the carrier lifetime, τ , instead of the quantum efficiency, η , which would occur if there are the two types of F-centers. He proposed that τ could be decreased by an increase in the concentration of halide

ion vacancies, which in turn, are produced by the optical destruction of F-centers. However, Markham failed to mention how this hypothesis could satisfy a major objection raised by Oberly against such an interpretation. Oberly (19, p. 1258) contended that a process resulting in the production of effective electron traps could not satisfactorily explain the decrease in the rate of photoconductive fatigue, or weakening, under prolonged illumination. Furthermore, since nearly all photoelectrons are trapped before reaching the anode region, it is difficult to envision how traps with larger cross sections could be produced by the preferential filling of traps having smaller cross section, as would be required by this viewpoint. The converse, the preferential filling of more effective traps resulting in the build up of less effective traps, is very plausible, but then only an enhancement in photoresponse rather than a weakening should result, since τ would thereby be increased.

This same viewpoint introduced by Markham was expanded by Nielsen and Scott (18, p. 300-303). Incidental to some other photoconductive measurements reported by them, a marked decrease in the F-band photoresponse was observed under F-light illumination, which

was attributed to a build-up of the negative ion vacancy concentration. A bleaching of 2×10^{15} F-centers, which was only about 5 per cent of the original F-center concentration, caused a photoresponse drop of 80 per cent. As pointed out by Nielsen and Scott, in order for this interpretation to be tested quantitatively, some prior knowledge of the halide ion vacancy concentration in the original unbleached crystal is required. This initial concentration must be considerably lower than the concentration of vacancies produced by bleaching to satisfactorily account for the much greater weakening of photoresponse as compared to the smaller drop in absorbancy. Nielsen and Scott reported a lack of any precise measurements or calculations that might furnish such information.

Any further attempts to resolve these controversial interpretations of the fatigue in photoresponse have not been reported in the literature. Indeed, it is rather surprising that these two opposing viewpoints have not incited a more thorough experimental investigation of the problem.

Objectives

The objectives of this investigation are: 1) To overcome the problem of space-charge polarization and secondary currents associated with D.C. photocurrent measurements of alkali halides (see page 11); 2) to determine quantitatively the loss in photoresponse observed by Nielsen (18, p. 299-300) of colored KCl aged in the dark for extended periods of time; 3) to critically examine the photoconductive fatigue observed in the F-band of colored alkali halides through a detailed study of the nature of the fatigue effect, itself, with measurements of any related phenomena. It is hoped that a better understanding can be had of the individual roles played by the quantum efficiency and by the average carrier lifetime in this weakening of the photoresponse (see pages 21-26).

II. EXPERIMENTAL PROCEDURE

Potassium chloride was chosen as being representative of the alkali halides because it has been the most thoroughly investigated member of this family, not only in color center work, but in other experimental and theoretical studies as well. Furthermore, as noted on pages 18-19, room temperature is well above the second thermal increase in photoresponse for KCl, so that the photoconductivity cell need not be equipped with a thermostatic enclosure as would be required for the other commonly encountered alkali halides, NaCl and KBr. Thus, all measurements were made on KCl at room temperature.

Sample Preparation

The bulk of the measurements were performed on portions of a single KCl crystal obtained from the Harshaw Chemical Company. Spectrographic analysis of the purity of similarly prepared KCl samples from the same company can be found elsewhere (2, p. 1044). Single crystals of KCl grown by the Kryopolous method from doubly-recrystallized reagent grade KCl were also employed. They were grown by others in this laboratory. A platinum-free ultra-pure crystal was generously supplied by P. Gruzensky, and divalent-ion-doped crystals were furnished by H. Coker and R. Watson.

In every case the crystals were colored additively by heating the crystal in a vapor of potassium metal. Another commonly employed coloration method, X-ray irradiation, was never utilized since the instability of the F-band produced by this coloring method would obscure photoconductive fatigue measurements. This instability is caused by the optical and thermal release of F-center electrons and their subsequent recombination with the original holes -- in this case neutral halogen atoms -- whereas such holes are not present in additively colored crystals. Moreover, with X-rayed crystals certain complications may arise from the unexplained low temperature F-band bleaching observed recently in X-rayed alkali halides (15, p. 762-771).

The crystals to be colored were wrapped in copper foil and placed in the upper portion of a Pyrex tube containing some potassium metal. The tube was then evacuated, sealed, and placed in a vertical double unit furnace, each unit having a separately controlled heating element. The upper unit, heating the crystals, was usually maintained at 500°C , while the temperature of the lower unit, being generally 100° to 200° lower, governed the vapor pressure of the metal vapor, and, therefore, the extent of coloration. Thermal treatments lasted from 12 hours to 72 hours, the longer times were

needed to produce uniform colorations at lower temperatures.

Quenching the colored crystal was accomplished by merely crushing the tube in a metal trough immediately after furnace removal. The colored crystals, still wrapped in their lighttight copper foil, were quickly recovered from the debris and cooled to room temperature in an air blast. Thirty to forty seconds were generally required for the entire quenching operation. In place of the air blast a carbon tetrachloride bath was tried, thereby reducing the quenching time to ten seconds, but this proved to be unsatisfactory due to the formation of several crystal cleavage planes caused by the sudden thermal shock.

Due to the very low light intensities used initially in photoconductive fatigue experiments, great care was needed to avoid exposing the samples to any stray illumination in the F-band region while preparing them for measurement. It was found that an ordinary photographic red safety lamp, used in the above quenching operation, emitted a significant amount of light in the long-wavelength tail of the F-band in KCl. An estimated 7 per cent of the total illumination of a General Electric safety lamp was contained in the wavelength region 560-610 m . This estimation was made using the

lamp as a light source in the monochromator-thermopile instrument to be described later.

Reproducible measurements were obtained only after replacing the red lamp with a specially designed F-light filtered lamp for the subsequent cleaving and mounting operations. Two superimposed liquid filters were used -- KMnO_4 and $\text{Cu}(\text{NH}_3)_4\text{SO}_4$ -- to produce a light source having better than 99 per cent of its illumination composed of wavelengths shorter than $490 \text{ m}\mu$ and longer than $620 \text{ m}\mu$. The solutions proved to be much less stable than was anticipated; requiring replacement after 20 minutes of operation. It was found more convenient, with some practice, to master the techniques of working in total darkness.

In order to be able to cleave the colored crystal in the dark to any desired dimension, a device resembling a miniature guillotine was employed. The crystal having been clamped in place on the base plate could be easily cleaved with one stroke on a razor blade held against two upright posts. The dimension selection could be preset under ordinary lighting before insertion of the crystal. A typical crystal used in photocurrent measurements would measure 5 mm. by 2 mm. by 1 mm. with the light impinging on, and the electric field traversing, the smallest dimension.

To mount properly the crystal in the photoconductivity cell, continuing to work in the dark, a removable sheet metal chute was found to be very helpful. Usually the crystals were washed in absolute ethanol before inserting in the cell to remove any surface layer of water. A dry atmosphere in the photoconductivity cell was maintained by means of magnesium perchlorate. With these precautions it was found that no observable surface conductivity occurred, making it unnecessary to evacuate the cell.

The same precautionary measures taken to ensure the total exclusion of any stray illumination for the photoconductivity samples were also heeded in the preparation of samples for optical measurement.

Optical Measurements

Bleaching and optical density measurements were conducted in a battery-operated Beckman spectrophotometer, Model DU. The crystals, being somewhat larger than those used for photoconductance measurements, were mounted on the back side of a supporting plate over a circular hole 2.5 mm. in diameter, being held in place with Cenco "softseal takiwax." Another identical circular hole, in air, served as a reference standard. A thermopile, to be described later, was used to obtain an absolute measurement of the light intensity at 560 m for various slit widths.

The concentrations of F-centers were calculated from optical density values through the use of the Smakula equation, setting the oscillator strength equal to unity and assuming a constant "half-width" as was done by Scott and Smith (31, p. 984).

Bleaching experiments were performed at 560 $m\mu$ by observing the rate of change of optical density with time, the crystal being left in its initial position under constant illumination. To expedite the accumulation of data, and also to minimize the effect of instrument drift, in the later stages of bleaching a "bleaching" intensity, several times more intense than the light

needed for measuring the optical density, was used between optical density measurements. With the shutter open, a warm-up period of at least 30 minutes was required for the instrument to attain its maximum stability.

Photoconductivity Measurements

Photocurrents of the order of magnitude of 10^{-11} amperes were amplified with a D.C. amplifier and were then read by either a built-in microammeter or a Brown recording potentiometer, Model 153X12V-X-9. The input of the recorder was connected to the center tap of a SPDT switch built into, and synchronized with, the shutter on the light source of the monochromator. By means of this synchronizing switch, the output of the amplifier would be fed into the recorder only when the photoconducting crystal was being illuminated; while the shutter remained closed, a constant, but variable, voltage from the second terminal of the DT switch would serve as the input, allowing any scale reading on the recorder to be selected before a measurement is begun. Then if some prior knowledge is had of the photocurrent to be obtained, the recorder pen could be preset at the value thereby reducing the pen lag considerably, especially for full-scale or nearly full-scale photocurrent readings. This facility proved to be a valuable asset in reducing extrapolation errors, to be discussed presently. This switch also provided a convenient way of measuring the exposure time accurately, since small jogs of the pen could be easily identified on the chart paper coinciding

with the opening and closing of the shutter, the chart speed being accurately known.

From the trace of the decaying photocurrent on the chart paper of the recorder -- the decay being due to the space charge polarization discussed on page 11 -- an extrapolation could be made to zero exposure time. These extrapolated values of the photocurrent were assumed to be the initial currents that would have been obtained in the absence of any space charge polarization or instrument response time, and were the values recorded in the data. A linear extrapolation, such as used here, can be justified on the basis that the photocurrent decays exponentially with exposure time, as was shown by von Hippel (38, p. 571-572), and the extrapolated region involves only a small exposure near zero time where an exponential curve would be approximately linear. In order to improve the accuracy of these extrapolations, the chart speed of the recorder was increased by a factor of 36 by inserting a high speed synchronous motor into the drive mechanism. Intermediate speeds could be obtained, as with the standard motor, by exchanging a few gears. This entire procedure will be referred to occasionally as the "synchronized recorder" method.

Graph 1 illustrates a typical chart-paper trace

obtained by this synchronized recorder method. Before starting the chart-drive mechanism, an electric field would be applied to the crystal. Beginning at time "zero" the KCl crystal would be illuminated, while, simultaneously, the recorder would leave its pre-adjusted position (line a) and begin to read the amplifier output by means of the shutter-synchronized switch. After a photocurrent trace for 3 seconds (curve bc), the shutter would be closed and the recorder returns to its pre-adjusted position (line a'). The dotted line, d, is the extrapolation mentioned above. Curve e represents a photocurrent trace to be expected in the absence of any space charge polarization. Curve fc would be the trace obtained if the recorder had started from a zero position instead of the scale reading noted by line a in the diagram. In this case the instrumental lag, T_p , is due principally to the pen-drive mechanism. Since the pen began recording the true current at point P, T_i represents the delay due to a finite electrometer tube response time, always observed unless a faulty pre-positioning of the recorder results in a trace similar to that depicted by curve fc. An extrapolation of the curve fc would be difficult and inaccurate because of its curvature and distance from the origin.

As has become common practice for such D.C.

measurements, following each photocurrent measurement the crystal was depolarized by discharging the electrodes and illuminating the crystal as before. The photoelectrons now drift in the opposite direction under the influence of the field developed by the polarization itself, and thus the space charge is reduced. It was found that a depolarization period lasting four times as long as the preceding photocurrent measurement was needed for at least 95% space charge elimination. Depolarization exposure times were measured with a stop watch.

Although the above procedure effectively solved the polarization problem, it is limited to measurements having photocurrent lag times (see page 6) less than the instrument response time. Moreover, a single photoconduction fatigue determination would frequently involve as many as 50 such measurements, and require over two hours for its completion. A much less laborious procedure involved the use of a motor-driven switching device to be described later. This permitted measurement of photocurrents having very long lag times, since it was designed to operate with continuous rather than intermittent illumination.

The various components of the photoconductivity apparatus will now be taken up in greater detail.

Photoconductivity Cell. The design of the cell is shown in Plate 1. The light beam enters the cell via the window (1), illuminates the entire front surface of the photoconducting crystal (9), passes through the crystal, and is reflected by the rear mirror (8) causing the beam to pass through the crystal a second time. Provided that the crystal is not too intensely colored, this double pass of the light beam produces a more uniform absorption of light throughout the volume of the crystal. A calculation based on Beer's law shows that for a crystal thickness of 1 mm. in the direction of the light beam and an F-center concentration of 1×10^{15} cm. the light absorption at the front surface would be only 3% higher than that at the rear surface, whereas the same crystal using only a single pass would have a 39% discrepancy. The two side mirrors aid in preventing a scattering of the light beam. The brass cylinder (2) together with its lid (3) can be readily removed to insert a crystal. The whole unit is placed into its light-proof housing in front of the light beam by sliding the outer flange of the base plate (4) into a snugly fitting groove in the housing. A reproducible positioning of the crystal in the light beam can thus be readily achieved as was determined by several trial dismantlements. Not shown in the diagram are spring terminal clips

attached to the bolts (6) for the amplifier and high voltage connections, further simplifying the dismantling of the cell for darkroom loading. Also omitted from the diagram is a metal trough lying on the bottom of the cell and containing the magnesium perchlorate desiccant. The mirrors, carbon electrodes, glass window, cylinder lid, and the cylinder itself are all secured in place with Cenco "softseal takiwax". For the side mirrors and electrodes the wax was first mixed in the molten state with a small amount of finely divided graphite to render the wax moderately conducting.

The light-proof housing referred to above also houses the thermopile, so that either the cell or thermopile can be very conveniently slid in front of the light beam. Again, a reproducible positioning of either one is had by the snug fit of two holes in the housing wall over two screw heads in the monochromator slit assembly.

Thermopile. The thermopile, used for measuring light beam intensities, was constructed as described by Launer (11, p. 99-100), with the following modifications: 1) copnic-nichrome wires (B&S No. 36) were used in place of the Chromel-P and Constantan suggested, 2) 0.012 mm. tin sheeting was substituted for the silver for the receiver plates, 3) due to the space limitations,

nine receiving plates in two cascades were used instead of a total of 22, 4) black soot from a burning candle provided the blackening on the receiver plates, and 5) the junctions were soldered under a 5-power magnifying glass by use of a miniature soldering iron described by Forsythe (4, p. 194).

The outer vacuum-sealed casing was the original thermopile casing prepared by K. H. Sweeney in this laboratory. Identical microscope cover glasses served as windows for the thermopile and photoconductivity cell, eliminating the need for any "window" corrections for light absorption.

The electrical output of the thermopile was read from a Leeds and Northrup Type HS galvanometer from a scale two meters distant. The combined resistance of the thermopile and galvanometer amounted to 20 ohms, which is considerably less than that required for critical damping, but the galvanometer functioned satisfactorily nevertheless.

A calibration of the thermopile-galvanometer system was made with a calibrated carbon filament lamp obtained from the National Bureau of Standards. Calibrating instructions supplied with the lamp were followed very closely except that shorter lamp distances were needed to obtain a suitable light intensity. Use

of the inverse square relationship between lamp distance and light intensity was substantiated by several comparative measurements at various lamp distances. A Weston A.C. ammeter, Model 155, was used in the calibration, and was itself calibrated by calorimetrically measuring the heat produced across a resistor of known resistance. Operating in a vacuum, the thermopile had a sensitivity of 3.36×10^{-6} watts per centimeter deflection, while in air it was somewhat lower at 7.09×10^{-6} watts per centimeter deflection.

Monochromator. As a source of F-band illumination for these photoconductivity experiments, a double prism monochromator, constructed from the remnants of a demonstration model, proved to be quite adequate. The exit slit, together with its optical system, and the two prisms were fixed into position. A scan of the spectrum can be had by a rotation of the entrance slit and light source assembly about a pivot point aligned with the axis of the first prism. With the exit slit width set at 1.5 mm., the entrance slit width can be adjusted by means of a thumb screw having 120 scale divisions per mm. slit width. The optical system of a 35 mm. slide projector, including a 300 watt tungsten lamp, served as a light source. On the table near the light source a wavelength scale was installed.

Using neon and helium gas discharge tubes as light sources the wavelength scale of the monochromator was calibrated by comparing spectra observed with data given in the MIT wavelength tables (6, p. xix). The five most intense lines for each gas were identified and used in the calibration. These spectral lines were detected by eye in a darkened room using fairly narrow slit widths, never exceeding 0.5 mm. Then, as a check on the calibration, the light beam of the Beckman spectrophotometer was focused on the entrance slit of the monochromator and the wavelength region 300 to 800 $m\mu$ was scanned. Good agreement was obtained at all wavelengths except below 500 $m\mu$. Of primary importance, since all measurements were conducted in the F-band of KCl, the region around 560 $m\mu$ provided excellent agreement. Due to limitations imposed by the quality of the glass, the spectrum was limited to the visible region, 400 to 750 $m\mu$.

An estimation of the purity of the monochromatic illumination at various slit widths can be obtained from a comparison of the slit widths and the instrument dispersion as described in Hogness, et al. (7, p. 394-396). The linear dispersions at the entrance slit for the wavelength regions 400 to 500 $m\mu$, 500 to 600 $m\mu$, and 600 to 700 $m\mu$ are 14.5 mm., 11.3 mm., and 6.5 mm.,

respectively. Typical settings have the exit slit fixed at 1.5 mm. with the entrance slit ranging from 1.0 to 2.0 mm. Thus, for an entrance slit width of 1.0 mm. the expected wavelength spread of the monochromatic light beam would be 17, 22 and 39 m μ respectively, for the above three wavelength regions; and with an entrance slit width of 2.0 mm. these same spreads would be estimated at 24, 31 and 54 m μ . It is assumed here that any non-achromatism of the lenses has only a negligible effect on the purity of the dispersion. An examination of the broadening of the helium and neon line spectra with increasing slit widths yielded satisfactory agreement with these calculations.

Amplifier and Power Supply. Both the amplifier and power unit were constructed by G. Nielsen from a design given by Roberts (26, p. 181-183). Plate 2 is a simplified diagram of the amplifier circuit. Several modifications introduced will be described, and a brief description of the operation of these two units will also be given. A more complete discussion of the construction of the amplifier and its performance can be found in Roberts' original paper.

Only one modification was incorporated into the

power supply. On its chassis a rotary switch was installed to permit a selection of seven different voltages to be applied to the photoconductivity cell. Except for the maximum voltage, 450 volts, and the next lower voltage, 300 volts, all other consecutive switch positions gave voltages separated by no more than 50 volts. Intermediate voltages having a minimum 5 volt separation were obtained using a $22\frac{1}{2}$ volt battery, of either polarity and any 3 volt fraction thereof, in series with the rotary switch output.

This composite high voltage source was used primarily during a preliminary investigation of polarization effects to measure the polarization field generated by space charges. After a photocurrent drain produces some degree of polarization, the applied field needed to yield a null photocurrent would then be assumed to be equal, but opposite, to the polarization field. Using maximum current amplification, this polarization voltage could be measured to an accuracy of ± 3 volts.

In parallel with the electrodes of the photoconductivity cell was placed an oil-filled 4 microfarad capacitor having good storage characteristics. A constant voltage could then be had by first charging the capacitor and then disconnecting the power unit, thereby eliminating the voltage fluctuations of the power supply.

The small current drain through the photoconducting specimen during the course of a measurement causes only a negligible drop in the voltage of the capacitor. Provision was also made for a second capacitor in the circuit so that a higher voltage of 900 volts could be utilized.

Besides furnishing a high voltage for the electrodes, this same power unit supplied the tube filament voltages and 165 volts for the amplifier circuit shown in Plate 2.

Boosting the operating voltage from the recommended 150 volts to 165 volts effectively stabilizes the current with respect to line voltage fluctuations which cause a slow drift in gain. A large amount of negative feedback is incorporated in the circuit so that the gain, or amplification factor, is given simply by the ratio R_1 to R_2 , independent of the tube characteristics. With R_1 having a fixed resistance of 6.08×10^9 ohms, and R_2 a variable resistance between 600 and 6,000 ohms, gains varying from 10^7 to 10^6 could be obtained.

In order to minimize inductive pickup and ground loop disturbances while the DPDT motor-driven switch is in operation, it was necessary to move the ground point from position "G" to position "Lo", and to mount the electrometer tube inside of the amplifier cabinet,

shielded by its own metal envelope.

Other modifications include a switch, S_2 , inserted to prevent possible damage of the microammeter from current surges encountered occasionally in preparatory adjustments of the amplifier, and the voltage divider output circuitry used to feed the potentiometer through the shutter synchronizer previously described.

Controls near the upper edge on the top panel of the amplifier cabinet are, from left to right: R_5 , for bringing the record's scale readings in alignment with the microammeter, necessitated by the removal of the recorder's standardization mechanism; S_3 , for selecting either the microammeter or the recorder to measure the output without introducing a change in the amplifying characteristics; and the "off-on" switch, S_2 . A knob located in the lower left hand corner is used to minimize the output oscillations when the motor-driven switch is in operation (adjustment R_6 on Plate 4). The microammeter, itself, is mounted in the center of this same panel.

Mounted on the side panel, just as they were in Nielsen's original design, from left to right, are: S_1 , "off-on" switch for the entire circuit; R_4 , for "zeroing" the instrument; and two controls for obtaining three different amplification factors through the adjustment

of R_2 .

Motor-driven Switch. As stated earlier, one of the objectives of this investigation was to overcome the problem of space charge accumulation during photocurrent measurements. The synchronized recorder method proved to be rather laborious and limited in scope, although otherwise apparently quite successful. A mechanical switching device operating up to speeds of 20 cps was developed which would greatly expedite photocurrent fatigue measurements. Although introducing an alternating field on the photoconducting sample, the device was not intended for alternating current applications, having been designed for subsequent D.C. amplification.

The seemingly obvious use of a purely A.C. method to overcome polarization effects has not yet met with very much success. Relatively large electrode capacitances, inherent in the design of a sample holder for thin crystals, produce currents which are almost entirely reactive, even for frequencies as low as 20 cps. MacDonald (12, p. 294), working in the audio-frequency range, has circumvented this difficulty by employing a duplicate "dummy" sample holder to balance the bona fide sample holder in his capacitance bridge. However, while D.C. polarization effects are still not

too well understood in alkali halides, even less is known about space charges in A.C. measurements of these same crystals. At higher frequencies, where space charge polarization can be assumed to be absent, other uncertainties such as variable dielectric losses are encountered which make a correlation between A.C. photo-capacitive and D.C. photoconductive measurements very difficult in the light of our present knowledge. These problems associated with a purely A.C. method are believed to be absent in the design of this device when operating at frequencies not exceeding 20 cps.

Plate 3 shows the construction of the switch, and Plate 4 its circuit connections. The switch is driven by an eccentric cam (2) on the motor shaft (1), with the bearing (4) serving as a pivot for its oscillating motion. Omitted from the diagram are "Teflon" insulating strips under the terminal blocks (5), a counter operating off of the motor shaft (1) used to measure the speed of oscillating, and all electrical connections.

As can be seen from the switch representation on Plate 4 and the sequence of operations on page 96, vibrator B remains in the B_2 position while vibrator A executes its entire motion returning to the position A_1 . Then, while vibrator A remains in this position, vibrator

B undergoes its entire motion and returns to position B_2 . The cycle is then repeated.

In spite of this "out-of-phase" operation of the two vibrators, both spend nearly half a period in either of their two terminal positions. This is made possible through the use of thin spring metal moving parts which permit considerable flexing so that the entire switching operation requires less than 0.15 of the period. Better than 50% of this time, roughly 0.08 of a period, is spent with the vibrators in an $A_1 - B_2$ position. A more than adequate time allowance for this part of the switching operation not only ensures the proper sequence of events, but also permits ample time for the electrodes to become fully charged before the amplifier is engaged. Thus, the observed photocurrent should have no reactive component, unlike the largely reactive photocurrents obtained in a typical A.C. method.

A modified square-wave photocurrent signal would be the amplifier input expected from this device. The raised portion of the square-wave would correspond to the actual photocurrent, obtained when vibrator A is in the A_2 position, which comprises about 0.45 of the period. The remainder of the period the amplifier is in a "floating" position, where it is made to read a zero photocurrent through a previous adjustment of R_4 . It is

during this interval that the crystal depolarization takes place. Due to the slow electrometer tube response time, calculated to be 0.5 seconds, this square-wave input would appear as a nearly constant output having a magnitude equal to the time average of the hypothetical square-wave output that would be obtained with an infinitely small electrometer response time. Thus, the actual photocurrent should be the observed photocurrent multiplied by $\frac{1}{x}$, where x is the fraction of a period that A_2 is closed. Hence, it was necessary to accurately determine the value of x .

This was done with the switch operating at speeds ranging from 5 to 20 cps. The amplifier input was disconnected and in its place a capacitor and a load resistor were connected in series with the contacts A_2 . Then by observing the capacitor discharge time, first with the switch inoperative and A_2 closed, later with the switch operating, the value of x was calculated from the ratio of the former discharge time to the latter. x was found to be 0.38, independent of the switching frequency throughout this frequency range. Similarly, the time that the vibrator spends in the A_1 position was calculated to be 0.58 of a period. The remainder, 0.04 of a period, can be attributed to the vibrator transit time.

Considering the rather crude construction of this motor-driven switch it proved to be remarkably stable. It was necessary, however, to clean the all-brass contacts after one or two hours of use. While in operation, the application of a few drops of carbon tetrachloride to each contact would render them self-cleaning.

By far the most difficult installation problem was that of isolating and shielding the electrometer tube and its leads from the inductive effect of the high voltage electrode charging and discharging. The effect was noticed by large needle oscillations with the switch operating at very low frequencies. Various measures taken to reduce this effect are listed here in order of decreasing importance:

- (1) Triple Teflon insulation (6) separating the vibrating contacts as shown on Plate 3.

- (2) Grounding the shield (9) together with the shielding of the lead wires of switch "A" directly to the amplifier ground shown on Plate 2.

- (3) Removing the electrometer tube from its private compartment and placing it inside the amplifier cabinet close to the ground location.

- (4) Changing the ground location on the amplifier from terminal "G" to terminal "Lo".

(5) Isolating the shield (9) from its mounting with Teflon spacers.

(6) Positioning the entire switch as close as possible to both the photoconductivity cell and the amplifier so as to minimize the length of the connections.

(7) Grounding the shield of the amplifier-power supply connector midway between the two chassis.

(8) Then, using a separate connection to the water pipe ground, the following were grounded:

(a) The entire photoconductivity cell, including the sheet metal lid.

(b) The light-proof cell housing.

(c) The shield of the amplifier-power supply connector at both ends.

In spite of these elaborate measures to eliminate or compensate for inductive pickup and ground loops, a small residual oscillation was still observed. It was of sufficiently small magnitude that simply applying a very low voltage, on the order of a tenth of a volt, to contact A_1 would correct for it. This was done by adjusting R_6 of Plate 4 after having first zeroed the instrument through the adjustment of R_4 .

Polarization Field Measurements

After a photocurrent has been drawn from a KCl crystal leaving the crystal in a highly polarized state, a measure of the electric field strength generated by the polarization charges was obtained by the null photocurrent method. Proceeding first to remove the original applied field which produced the photocurrent, some intermediate voltage opposed to the polarization field would be selected from the composite power supply described on page 45. All such voltages were measured by a vacuum-tube-voltmeter. The light beam would then be flashed onto the crystal through a rapid movement of the shutter, and the direction and magnitude of the microammeter needle swing would be noted. Higher or lower voltages would be selected accordingly, until no photocurrent could be observed when the light beam was flashed. Polarization voltages in the range of 0-300 volts could be determined with an accuracy of ± 3 volts.

An important advantage of such a null current method is the negligible disturbance of the space charge due to the very short current pulses drawn from the crystal in the course of these measurements.

III. EXPERIMENTAL RESULTS

Photoconduction Fatigue

A brief introduction to the method employed will help to clarify the experimental findings. The procedure for obtaining individual photocurrent measurements has already been fully described on pages 35-37 and illustrated by graph 1. The three "blips" shown in figure b of graph 5 are the same such measurements, here represented on a greatly reduced scale. For simplicity, the recorder is shown in every case to start from "zero", while in reality this was always avoided experimentally for the reason mentioned on page 26. In figure a of the same graph the "on-off" periods of the light beams (I), and the electric field (E) are shown. It is to be observed that a complete cycle of I and E adjustments accompanies each photocurrent measurement. The significance and importance of the location and length of each interval within the cycle will become obvious in the following two sections; it suffices here to note that the crystal's exposure to light consists of the depolarization period, interval I, together with the photocurrent measurement itself, interval III. A photoconductive weakening, or fatigue, in successive cycles is illustrated by the Δi notations.

Since any exposure to F-light has been found to have the same diminishing effect on photoresponse, irregardless of whether or not an electrical field is applied to the crystal and a photocurrent is drawn, it would perhaps be more appropriate to refer to the above phenomenon as a photoconductivity weakening due to previous illumination, rather than a photoconduction fatigue. There is another objection that can be raised against the use of the term "fatigue" in that no recovery of photoresponse was ever observed in these crystals even after their remaining in the dark for as long as 48 hours. Although somewhat ambiguous, the word "fatigue" was nevertheless preferred to other more descriptive terms.

Graph 6 depicts the results of a typical fatigue experiment. The abscissa, It , is the number of quanta absorbed per cubic centimeter, obtained by adding together all of the absorbed quanta of preceding cycles, t being the time, and I the rate of absorption, quanta per cubic centimeter. I/I_0 , according to the development given equation (5) on pages 5 and 6, is directly proportional to the photoresponse. The crystal employed for this experiment had an F-center concentration of $6.9 \times 10^{16} \text{ cm}^{-3}$. Nine other crystals, from three different coloration samples of the same Harshaw KCl, gave very nearly identical fatigue curves.

In complete agreement with the findings of Oberly (19, p. 1258), the fatigue rate, starting at a considerably high level, undergoes a very marked decrease with continued illumination. Not reported by him, however, was a "leveling off" of the fatigue curve resulting in a constant, non-zero, photoresponse after prolonged illumination. The particular crystal sample from which the data in graph 6 was obtained displayed an additional 30% decrease in photoresponse beyond the residual values shown in graph 6 after a much larger exposure to $I t = 2.5 \times 10^{19} \text{ cm}^{-3}$. Thereafter, a second $2.5 \times 10^{19} \text{ cm}^{-3}$ exposure produced no noticeable change in photoresponse. Thus, if the photoresponse does approach zero asymptotically, it does so at an extremely low rate.

Show in graph 7 are four KCl samples differing in purity, and having approximately equal F-center concentrations, N_F^0 . The parameters plotted here are identical to those in graph 6 except that a logarithmic plot was needed on the ordinate so that all four curves could be compressed onto the same graph for comparative purposes.

Optical Bleaching

Mainly in support of the discussion to follow in Part IV, some bleaching measurements were made. The simple procedure has already been discussed.

In every case the specimens were cleaved from the same crystal samples as were the photoconductivity specimens. Graphs 8 and 9 are representative of the results obtained. The ordinate for these graphs is a measure of the fraction of F-centers bleached. N represents the number of F-centers bleached per cubic centimeter, while N_F^0 is the initial F-center concentration. This fraction is related to the experimentally determined absorption coefficient, α , by the equation

$$N/N_F^0 = \frac{\alpha_0 - \alpha}{\alpha_0}$$

arrived at by assuming a direct proportionality between N_F and α , noting that $N = N_F^0 - N_F$.

Graphs 6 and 8 are of the same colored KCl sample. Likewise, graphs 7 and 9 compare the photoconduction fatigue and optical bleaching of the same four samples. It is to be noted that these bleaching curves extend over a much smaller range of I values than do the photoconduction fatigue curves. The Beckman spectrophotometer is not ideally suited for measurements beyond this range because of the low light intensity necessitating very

long exposures which are generally accompanied by large instrument drifts. A few measurements were made, however, beyond the range shown in graph 8, and results in a gradual bend downward beyond $I_t = 15 \times 10^{16} \text{ cm}^{-3}$, shown as point R on graph 6.

The curves of graphs 8 and 9 generally consist of two linear portions joined by a curved region, or "knee". The exception is curve B, which was observed to be nearly linear throughout its entire length.

Space-Charge Polarization

Since some knowledge of space-charge phenomena occurring during photocurrent measurements is needed to establish under what conditions polarization has a negligible effect on the data obtained, this preliminary investigation was undertaken. The same instrumental approach was followed for these measurements as was outlined for the synchronized recorder method, the Brown recording potentiometer again being used to produce a record of the rapidly decaying photocurrent. Polarization field strengths were measured as described in Part II. Graph 2 shows the results of three measurements, differing only in the magnitude of the applied voltage and, more significantly, in the time of exposure.

Although not clearly evident in graph 2, the photocurrent decay was found to be very nearly exponential, but only in the initial stages of decay. The dotted lines in graph 2 represent expected exponential extrapolations of the initial portion of the curves. In addition to the marked departure from exponential behavior after the passage of about 5×10^{-10} coulombs, polarization field strengths observed at the conclusion of the measurements (E_p in Table 1) were markedly different from those calculated on the assumption

of complete charge separation -- that is, for the entire space charge localized near the electrodes -- together with a graphical integration of the current vs. time curves shown in Graph 2. These results are presented in Table 1. It can be seen that for curves B and C the calculated field strengths were considerably higher than the corresponding observed values; and the longer the exposure, the greater the discrepancy. Only in the case of curve A was a fair agreement obtained between theory and experiment.

For charge passages not exceeding 7×10^{-10} coulombs, it was found that a depolarization period four times as long as the interval during which the photocurrent was measured was required for at least 95% depolarization. For larger charge passages, a multiplying factor somewhat smaller than four would suffice. These approximate results were obtained by observing when the polarization field reduces to 5% of the original applied field strength, and also by observing, through a series of photocurrent measurements following successively longer depolarization times, when the photocurrent is restored to within 5% of its original value. Obviously these latter measurements had to be performed on crystals that had assumed a stable photoconductivity after a previously induced fatigue in photoconductivity.

In view of the above findings it is not surprising that polarization fields were observed when the motor-driven switch was employed. Because of physical limitations in the design of the switch, a depolarization time interval could not be adjusted to be much greater than twice the photocurrent interval. When installed, this time ratio was set at $0.58/0.38$ or 1.5 as noted on page 51. It can be seen from Table 2 that a polarization field strength is quickly achieved and remains at that value throughout the measurement. To evaluate the data, this E_p must be subtracted from the applied field strength. The presence of this polarization field is unfortunate, however, because a complete charge separation must be assumed in order to validate this simple subtraction; and the postulate of complete charge separation has not been established with certainty.

Photocurrent Lag Time

It was noted on page 13 that colored alkali halides have not been known to exhibit a measureable photocurrent lag time at temperatures above the second thermal rise in photoresponse. For KCl, room temperature is well above this region. Therefore, when a greatly extended rise time, much longer than T_1 in graph 1, was observed while working with the motor-driven switch and employing continuous illumination, it was at first believed to be due to some additional instrumental effect. Later, an experiment was devised that verified the existence of a photocurrent lag time of about 40 seconds by eliminating the possibility of instrumental lag.

This experiment is illustrated in graph 3. Once again, the crystal was first subjected to a fatigue measurement so that its photoconductivity could be considered to have attained a stable value. The diagrams a, b, and c do not represent experimental observations, but are merely assumed free electron concentrations, N_e , at various time intervals and were included only as an aid in the interpretations of the photocurrent measurements. Three individual photocurrent traces, obtained by the synchronized recorder method, are shown by diagrams

d, e, and f. All three exhibit the typical polarization decay described on page 25. For simplicity, the recorder is shown in every case to start from "zero", while in reality this was always avoided for the reason mentioned on page 26. The three segments into which each diagram is divided are from left to right: a 2-minute depolarization period during which the crystal is illuminated under zero field; a variable dark interval, t_D , with the field applied ten seconds after the start of this interval; and a photocurrent interval that utilizes the same light intensity as was used during the depolarization period. The increased photocurrents (shown as Δi) are believed to be due to the residual concentration of photoelectrons (shown as ΔN_e) released during the preceding depolarization period.

Graph 4 shows a plot of data such as is presented in d, e, f; in this case the photocurrent is shown as a function of t_D . The 40-second lag time quoted above was obtained from this graph by noting the time needed for the current to decay to $\frac{1}{2}$ of the difference between its original and final values, according to the definition of lag time previously given. The original value was estimated by an extrapolation to $t_D = 0$. In addition, the final value of the photocurrent approached after very long dark intervals (i_∞ in graphs 3 and 4) also

was estimated to have the value shown in graph 4.

As stated earlier, photocurrent lag was initially believed to be due entirely to an instrumental lag. From the discussion given on page 6, based on a consideration of equation (4), it is to be noted that a photocurrent lag is merely another manifestation of a time lag in N_0 . Now, since the effect has been observed during a time interval in which the instrument is not in operation, it can be concluded that it is not of instrumental origin and that the above interpretation is correct.

A more detailed study of lag times in various crystal preparations was not attempted because of the unavailability of a better method of measurement. A definite rise time was noticed, however, while conducting every photoconduction fatigue measurement. This was manifested by a markedly lower initial reading -- undoubtedly due to the absence of a preceding illumination period -- than the succeeding few readings. Further, if the light intensity were increased during a series of measurements, the first reading after the increase was also lower than succeeding readings.

The presence of this photocurrent lag emphasizes the need for a measuring technique employing continuous rather than intermittent illumination and affixes some

doubt to the validity of the synchronized recorder method described on page 24. The overall effect was partially overcome by consistently using only 20-second dark intervals, with zero field applied to the crystals for the first ten seconds. Before this standardization of the dark intervals, poor reproducibility in fatigue measurements proved to be a major difficulty. This is not at all surprising in the light of this experiment. Reference to graph 4 reveals the fact that all photocurrents observed with a 20-second dark interval should be increased by about 50% to obtain the true values.

Aging

To test the effect on photoresponse of aging colored crystals in the dark at room temperature, a few measurements were made on crystals cleaved from the same colored sample at various times after coloration. The experiment was repeated later using another freshly colored sample. The results are summarized in Tables 3 and 4. No definite change in the initial photoresponse before fatigue was observed. However, the residual photoresponse following fatigue generally shows a very slight increase with age. The data furnished here is rather meager, so that this trend towards higher photoresponse could be due to some factor other than aging. Additional aging studies at different coloration and storage temperatures would, perhaps, better establish any such trend.

The better than 50% reduction in photoresponse observed by Neilson (18, p. 298) could have been caused, not by aging, but by accidental exposure to stray illumination. As mentioned under "Sample Preparation" difficulty was encountered in obtaining reproducible photoconductive measurements when the crystals were handled under the illumination of a red safety lamp. It is quite possible that some of the "older" crystals used by Nielsen had been exposed to longer doses of red lamp

illumination, or even room light, than the "fresher" sample he prepared later.

Performance of Motor-driven Switch

A major problem associated with this investigation has been the development of a device that would allow continuous photocurrents to be drawn in the presence of a constant polarization field which should be reduced to some very small value. Reference to table 2 reveals a polarization field that did appear to remain constant, but was not very small, being about one-third of the applied field strength in magnitude. The effective field strength in which the photoelectrons migrate is then the difference between the applied field and the polarization field, or two-thirds of the applied field. The reasons for the existence of such a large polarization field, as well as the danger inherent in subtracting it from the applied field in order to obtain an effective field strength, were mentioned on page 66.

Taken together, both the polarization reduced field strength and the "on" fraction of the switch cycle (the quantity x , page 51) would be expected to reduce the observed current to a fraction, 0.225, of the current that would be obtained by the synchronized recorder method. The actual fractional reduction was found to be 0.018, a much lower value. Normally, maximum photocurrent amplification is required even for measurements performed by the synchronized recorder method. Thus, although an

increase in light intensity could partially compensate for the expected fractional reduction in photocurrents of 0.225, a 60-fold increase was not feasible.

It is believed that this much larger reduction in photocurrent than was anticipated is due to a photo-capacitive effect, similar to that observed by MacDonald (13, p. 381), causing a greatly increased inductive pick-up in the electrometer circuit. This is in keeping with the observation of a consistently increased amplifier output as the shielding measures mentioned on pages 52 and 53 were introduced one at a time, and by the presence of a small residual fluctuation even after these elaborate shielding precautions were taken. It is quite possible that a more efficient shielding of the electrometer tube and its leads would eliminate the large reduction in photocurrent.

Pieces of glass and bakelite, carefully cleaned by vapor-rinsing first in steam and then in carbon tetrachloride, were mounted in the photoconductivity cell in place of the KCl crystal in an effort to determine whether the cause of the greater than expected reduction in observed photocurrent is associated with the photoconducting material as suggested in the above paragraph, or whether it is instrumental in origin. Operating at field strengths no greater than 5 volts/mm. the dark

currents produced by the motor-driven switch method and the synchronized recorder method differed by the expected value, the value of x , or 0.33. This would indicate that the supposition stated in the previous paragraph may be correct. Unfortunately, however, high electric fields such as those normally used for photoconductive measurements, produced very unstable currents in these materials, so that a measure of the reduction factor was impossible.

Hence, the problem remains unsolved. All of the data reported was obtained by the synchronized recorder method.

IV. DISCUSSION AND CONCLUSIONS

Theoretical Development

The mechanism favored in this treatment attributes the decrease in photoresponse following F-band illumination at a diminishing photoelectron lifetime caused by the illumination-induced generation of trapping centers of larger cross section than those which are being replaced. This can be realized if, when an F-center electron is released and becomes trapped, it leaves behind a halide ion vacancy which has a larger cross section for a subsequent trapping of another photoelectron than the original trapping center. The net result of this event is the loss of one F-center and a replacement of a halide ion vacancy for one trapping center, of which there are assumed to be at least 10^{16} cm^{-3} in the virgin crystal. These latter trapping centers will be frequently referred to as "thermally-stable traps", and are not to be confused with halide ion vacancies which are, themselves, very effective electron traps, and are also thermally stable. In addition to the trap-replacement feature, this mechanism assumes the conventional model of the F-center where all F-centers are identical and display unit quantum efficiency. This trap-replacement mechanism appears to have been originally proposed by

Markham (16, p. 433).

In consistency with the terminology introduced earlier (page 1) these halide ion vacancies formed by the release of electrons from F-centers should be referred to as "holes". This term will be avoided, however, because of the very likely possibility of some of these "holes" being present in the virgin crystals. Neither equation (2) nor any other subsequent relationship will permit such a definition of the term "hole". There is yet another reason for avoidance of the term "hole", as a more usual kind of hole in irradiated alkali halides exists at a photochemically generated free halogen atom.

All symbols used in this treatment are defined on page 78.

For a condition of dynamic equilibrium, the number of electrons trapped per second must equal the rate at which they are being formed, F. Thus, the rate at which the original trapping centers are being replaced by halide ion vacancies can be given by

$$\frac{dN(t)}{dt} = F \cdot \frac{S_t N_t}{S_t N_t + S_h N_h} = F \cdot \frac{S_t [N_t^0 - N(t)]}{S_t (N_t^0 - N(t)) + S_h [N_h^0 + N(t)]}$$

Several simplifying assumptions are needed to eliminate certain complexities in the mathematical

development of the above equation. N and F are assumed to be space-independent and F is also taken to be time-independent. Since the use of a double-pass of the light beam, together with fairly low F-center concentrations, produces a moderately uniform excitation rate, F , and therefore also a uniform N , throughout the volume of the crystal, the assumed space-independency of N and F seems justifiable. Regarding the time-independency of F , a somewhat more serious problem is encountered, since the effect cannot be minimized by a judicious choice of F-center concentrations as was the case for the space-dependency. In any event, the decrease in F with time, although in itself significant, as shown by the bleaching experiments, is never more than about 20%. It is hoped that before many more studies are based on this model, an exact treatment, where both F and N are treated as being space and time dependent, will be available.

Proceeding, then, with the integration of this equation

$$\left(1 - \frac{S_h}{S_t}\right) N(t) - \frac{S_h}{S_t} (N_h^0 + N_t^0) \ln \left[\frac{N_t^0 - N(t)}{N_t^0} \right] = F t$$

Assuming, now, that S_h is much greater than S_t , and that we are dealing with the region of very low exposure where N_t^0 is much greater than N , this integrated equation reduces to

$$N(t) \cong \frac{S_t N_t^0}{S_n N_n^0} Ft \quad (11)$$

If, instead, we are concerned with the region of very long exposure where N_t^0 is approximately equal to N , then

$$\ln \left[\frac{N_t^0}{N_t^0 - N(t)} \right] \cong \frac{S_t}{S_n (N_n^0 + N_t^0)} Ft \quad (12)$$

Considering next equation (1), we have very shortly after the continuous illumination is turned on, assuming no thermally unstable traps to be present

$$1/\tau^0 = \nu \left[S_n (N_n^0 + N_d^0) + S_t N_t^0 \right]$$

and after N thermally-stable traps have been replaced by halide ion vacancies

$$\begin{aligned} 1/\tau &= \nu \left\{ S_n [N_n^0 + N_d + N(t)] + S_t [N_t^0 - N(t)] \right\} \\ &= 1/\tau^0 + \nu \left[(S_n - S_t) N(t) + S_n (N_d - N_d^0) \right] \end{aligned}$$

It can be shown from the observed photoconductivity, using equation (4) and an estimated value of $10 \text{ cm}^2/\text{volt-sec}$ for (28, p. 367-368), that N_e never exceeded 10^6 cm^{-3} in any of the measurements reported here, while from the bleaching data N is found to exceed 10^{15} cm^{-3} almost immediately after illumination, so that the last equation written above can be simplified to

$$1/\tau \cong 1/\tau_0 + \nu (S_h - S_t) N(t)$$

Now introducing equation (5), noting that here $\nu = 1$ and $I = F$

$$F/\phi \cong (F/\phi)_0 + \frac{\nu}{e\mu} (S_h - S_t) N(t) \quad (13)$$

After prolonged illumination it can be assumed that N approaches N_t^0 when the trap replacement becomes nearly complete, so that

$$(F/\phi)_\infty \cong (F/\phi)_0 + \frac{\nu}{e\mu} (S_h - S_t) N_t^0 \quad (14)$$

Finally, eliminating N from equations (11) and (13) we have

$$F/\phi \cong (F/\phi)_0 + \left[\frac{\nu S_t N_t^0}{e\mu S_h N_h^0} (S_h - S_t) \right] F t \quad (15)$$

which predicts a straight line plot of F/ϕ vs. Ft in the region of low light exposure. Further, eliminating N_t^0 and N from equation (12) by combining it with equations (13) and (14) we then have

$$\ln M = \left[\frac{S_t}{S_h (N_h^0 + N_t^0)} \right] F t \quad (16)$$

for the region of very long exposures, where M is a

function of F/σ defined on page 78.

An alternative model for the fatigue in photo-response, that of Oberly, requires the assumption that S_t is equal to S_h . This results in a constant τ during bleaching. The photoconduction fatigue is then explained by assuming the presence of hard and soft F-centers. The bleaching rate can be expressed as

$$\frac{dN_F(t)}{dt} = -I \frac{N_S(t)}{N_F(t)} = -I \frac{N_F(t) - N_H}{N_F(t)}$$

which can be integrated, as before, to yield an equation analagous to equation (11)

$$N(t) = \frac{N_s^0}{N_F^0} I t \quad (17)$$

Generalizing to include the possibility that the hard centers are not completely hard and the soft centers are not completely soft, equation (17) becomes

$$N(t) = \left[(\eta_s - \eta_H) \frac{N_s^0}{N_F^0} + \eta_H \right] I t \quad (18)$$

Symbols Defined

Subscript or superscript "o" refers to the beginning of an illumination period; subscript " " refers to an indefinitely long illumination period. All concentrations and rates are to be considered on a per-unit-volume basis.

$$N(t) = N_F^0 - N_F(t)$$

= number of traps replaced by negative ion vacancies, after an illumination period of duration t; also number of F-centers bleached.

$$N_F = \text{F-center concentration.}$$

$$N_t = \text{thermally-stable trap concentration.}$$

$$N_h = \text{halide ion vacancy concentration.}$$

$$N_e = \text{equilibrium concentration of photoelectrons.}$$

$$N_s = \text{concentration of soft F-centers.}$$

$$N_H = \text{concentration of hard F-centers.}$$

$$S_t = \text{capture cross section of trapping centers for electrons.}$$

$$S_h = \text{capture cross section of halide ion vacancies for electrons.}$$

$$\eta_s = \text{quantum efficiency of soft F-centers.}$$

$$\eta_H = \text{quantum efficiency of hard F-centers.}$$

$$M = \left[\frac{(F/\sigma)_\infty - (F/\sigma)_0}{(F/\sigma)_\infty - (F/\sigma)} \right]$$

I = rate of quantum absorption.

F = rate of photoelectron production.

σ = conductivity.

Fatigue and Bleaching

Interpretation of Results. To test the validity of equations (11), (15), and (16) of Part IV, various plots of the data obtained from the Harshaw KCl are recorded on graphs 8 through 12. Excepting the previously described "knee" of the bleaching curves of graphs 8 and 9, the behavior predicted by the above mentioned equations was observed. It appears that Oberly proposed the multiple F-center model largely because he felt that the decreasing rate of photoconduction fatigue could not be explained by this more straightforward interpretation. The results of this investigation prove that the fatigue phenomenon can be explained adequately using a conventional model of the F-center, and that a more elaborate interpretation is not needed.

If the conventional model is correct, there remain certain photoconductive data reported in the literature which would require some explanation. One of the most puzzling is the remarkably stable photoresponse of the N and R-bands reported by Oberly (19, p. 258 and 1, p. 217). Since this model attributes the photoconduction fatigue to a build up of more effective electron traps, it is perfectly reasonable to expect a weakening of the photoresponse following F-light illumination, not only in the F-band, but in all of the various absorption bands,

it being assumed that electrons are the charge carriers produced in every case. The M-band does display such a diminished photoresponse after F-light exposure, but not the N and R-bands. Admittedly, this stability of photoresponse of the latter two bands is evidence against the mechanism postulated here.

On the other hand, the M-band diminished photoresponse following either F or M-band illumination can be fully explained according to Markham's model by assuming that both electrons and negative ion vacancies are produced by the optical destruction of either center. To explain this weakening of the M-band photoresponse using the multiple center model, Oberly suggested that the M-band also consists of hard and soft centers and that the soft M-center must have a companion absorption peak under the F-band. Perhaps unknowingly, he cited some data which affixes some doubt to the validity of his own theory. He reported that during F-band bleach the M-band photoresponse diminishes, but at the same time the absorption peak of the M-band increases. It is very difficult to explain this latter phenomenon from Oberly's viewpoint.

Although the data presented here cannot be considered a proof of the correctness of Markham's interpretation, it has furnished some evidence of a

contradictory nature concerning Oberly's model. Using the multiple-center interpretation, the existence of a very small residual photoresponse following prolonged bleaching or fatigue can be explained only by assuming that the hard centers actually have an appreciably non-zero quantum efficiency. In some instances, curve B of graph 7 particularly, the residual photoresponse was found to be quite significant. Allowing for a residual photoresponse by assigning some "soft" character to the hard centers would, however, only delay the approach to a nil photoresponse. Neither the results obtained here, nor those reported recently on high frequency measurements (12, p. 290), give any indication that the photoresponse does eventually approach zero. Another discrepancy can be noted. Table 5 shows a comparison of the slopes of the bleaching curves shown in graphs 8 and 9 with the theoretically determined rates using equations (17) and (18), and assuming that the rate, N_S^0/N_F^0 , could be approximated by $\alpha_0 - \alpha_\infty / \alpha_0$ from the bleaching data, since α , the absorption coefficient, and N are proportional. For equation (18), values of 0.8 and 0.2 were arbitrarily chosen for η_S and η_H , respectively. It can be seen that in the use of either equation a poor agreement with experiment is obtained. The experimental values are believed to be no more than 20% inaccurate.

Before leaving this subject, it is worth noting that the rapid bleaching rates observed here have been investigated recently by others (36, p. 1591-1594 and 12, p. 288-290), and in both instances the bleaching was accounted for on the basis of a limited concentration of effective electron traps being present in the untreated crystal. Their experiments did not include any photo-conductive measurements, however.

Trap Concentrations and Cross Sections. A number of estimates can be made by evaluating the slopes of the lines obtained from graphs 8 through 12 and a few additional graphs not shown here. Beginning with graphs 8 and 9 and equation (11), initially treating only the data on the Harshaw KCl, the slopes of the lines can be compared to the proportionality factor of equation (11) enclosed in brackets. Next, a similar comparison can be made between the slopes in graph 10 and the bracketed factor of equation (15). It is to be observed that a ratio of these two factors in equations (15) and (11) may be written as

$$\frac{(15)}{(11)} = \frac{\nu}{e\mu} (S_h - S_t)$$

so that a ratio of a slope from graphs 8 or 9 to one obtained from the curves in graph 10 should yield an

estimate of S_h when this slope ratio is equated to the above expression, assuming that S_t is negligible compared to S_h . Unfortunately, the value of μ and v are known only within about one order to magnitude, the values chosen for these calculations were $10 \text{ cm}^2/\text{volt-sec}$ and 10^7 cm/sec (28, p. 414), respectively.

N_t^0 can be approximated on the basis that it is at least as large as the number of F-centers bleached per cm^{-3} , which can be calculated from the product of $\alpha_0 - \alpha_\infty / \alpha_0$ and N_F^0

Having evaluated N_t^0 and S_h for either Harshaw sample, S_t can be calculated from the slopes of graphs 11 and 12 by equating these slopes to the bracketed factor of equation (16), assuming that N_t^0 is much greater than N_h^0 .

Finally, knowing the values of S_t , N_t^0 , and S_h , the value of N_h^0 can be calculated from the slope of the optical bleaching and the bracketed proportionality factor of equation (11). In all cases N_h^0 did in fact turn out to be much smaller than N_t^0 , justifying the assumption above.

These computations were also performed on the data obtained from K_2SO_4 and SrCl_2 -doped KCl , and the results are summarized in Table 6.

Contrary to expectations, the markedly different

photoconductivity performance of the various doped and pure samples appears to be due to differences in the cross-section of traps rather than their concentrations. The assumptions made concerning μ and v , together with the error-multiplication of the numerous steps in the calculation, render these values quoted here quite inaccurate, however. The inclusion of two significant figures in Table 6 can hardly be justified. However inaccurate, at least the non-conformity of the S_h values to some constant value demonstrates that the actual fatigue mechanism is more complex than this simple trap-exchange model would indicate. The computed value of N_h^0 is in good agreement with the lower limit estimation quoted on page 91.

The very interesting fatigue and bleaching curves of the ultra-pure KCl might be explained as follows. The overall trap concentration must be significantly lower to account for the much larger photoresponse, and the few traps initially present, which are responsible for the observed bleaching, must have nearly the same cross section as do negative ion vacancies in order to explain the absence of a photoresponse fatigue during the early stages of exposure. The eventual fatigue after long exposure could be attributed, perhaps, to a gradual production of electron traps by some migratory process

within the crystal. This is certainly worthy of further investigation.

The choice of SrCl_2 and K_2SO_4 as intentionally added impurities was based on the commonly held viewpoint that when divalent impurities enter substitutionally the crystal lattices of the monovalent alkali halides they must generate equivalent numbers of ion vacancies -- positive ion vacancies in the case of SrCl_2 , and negative ion vacancies with K_2SO_4 -- in order to maintain a charge neutrality in the bulk of the crystal. A high concentration of positive ion vacancies precludes anything but a low concentration of negative ion vacancies, provided an equilibrium of the two types of vacancies with vacancy pairs can be assumed. Thus, according to the trap-replacement mechanism described here, the SrCl_2 -doped KCl would be expected to give a higher initial photoresponse and faster photoconduction fatigue and bleaching rates than the "pure" KCl, due to the presence of a lower N_h^0 in the SrCl_2 -doped KCl. Likewise, a higher N_h^0 in the case of K_2SO_4 -doping would be expected to produce a lower initial photoresponse and slower fatigue and bleaching rates than the "pure" KCl. A comparison of curves B, C, and D of graphs 7 and 9 shows, in fact, that these effects were observed, but the seemingly obvious conclusion that these observed differences can be explained as outlined

above should be made with considerable reservation. For one, the calculations summarized in Table 6 do not show the expected differences in N_h^O . Secondly, the marked difference between curves A and C of graph 7 points out the need for using a single source of a purer form of KCl. Although colored under the same conditions, all four crystals that went into making graph 7 were prepared by different workers undoubtedly under different growing conditions so that differences in the concentration and distribution of lattice defects could very easily alter the concentration of both N_h^O and N_t^O sufficiently to account for the effects observed here. This is also worthy of further investigation.

Space Charge Polarization

A simple theoretical treatment described by von Hippel et al. (38, p. 571-572) predicts an exponential photocurrent decay due to the accumulation of polarization charges if confined to thin surface layers near the electrodes. As noted in Part III, at least initially the observed polarization decay is exponential, so that it is believed that the linear extrapolation to zero time is an accurate evaluation of what the photocurrent would be in the absence of any polarization. The later departure of the decay from exponential behavior, as illustrated in graph 2, can be explained on the basis of secondary currents, arising from field emission across the "space charge-electrode" double layer, contributing to the observed photocurrent. A loss in space charge following field emission would also account for the much lower observed polarization field strengths (E_p) than those calculated from von Hippel's model.

Since polarization fields commonly observed when the motor-driven switch was employed were found to be only about one-third of the applied field strength in magnitude, and since secondary currents appeared to occur only after the polarization field was built up to at least $\frac{1}{2}$ of the applied field strength, it is believed that photocurrents observed with the switch operating

have little, or no, secondary components.

Photocurrent Lag Time

Following the discussion given on pages 7 and 8, a comparison of the rise or decay time with the electrons' average lifetime, τ , should yield a lower limit to the concentration of shallow traps responsible for the photocurrent lag. The steady-state concentration of shallow-trapped electrons, N_e' , can be calculated from

$$N_e' \cong N_e \cdot \frac{L}{\tau} \quad (19)$$

where L is the observed photocurrent lag time and N_e the equilibrium concentration of conduction electrons.

Introducing equation (3), equation (19) then reduces to

$$N_e' \cong LF \quad (20)$$

For the crystal illustrated in graph 4, $L = 40$ sec., $F = 4 \times 10^{13}$, $N_e' = 1.6 \times 10^{15} \text{ cm}^{-3}$. This is the equilibrium concentration of shallow-trapped electrons and represents a lower limit of the shallow-trap concentration. An attempt to evaluate the actual concentration could be carried out by determining how large an F is needed to achieve a saturation of N_e' .

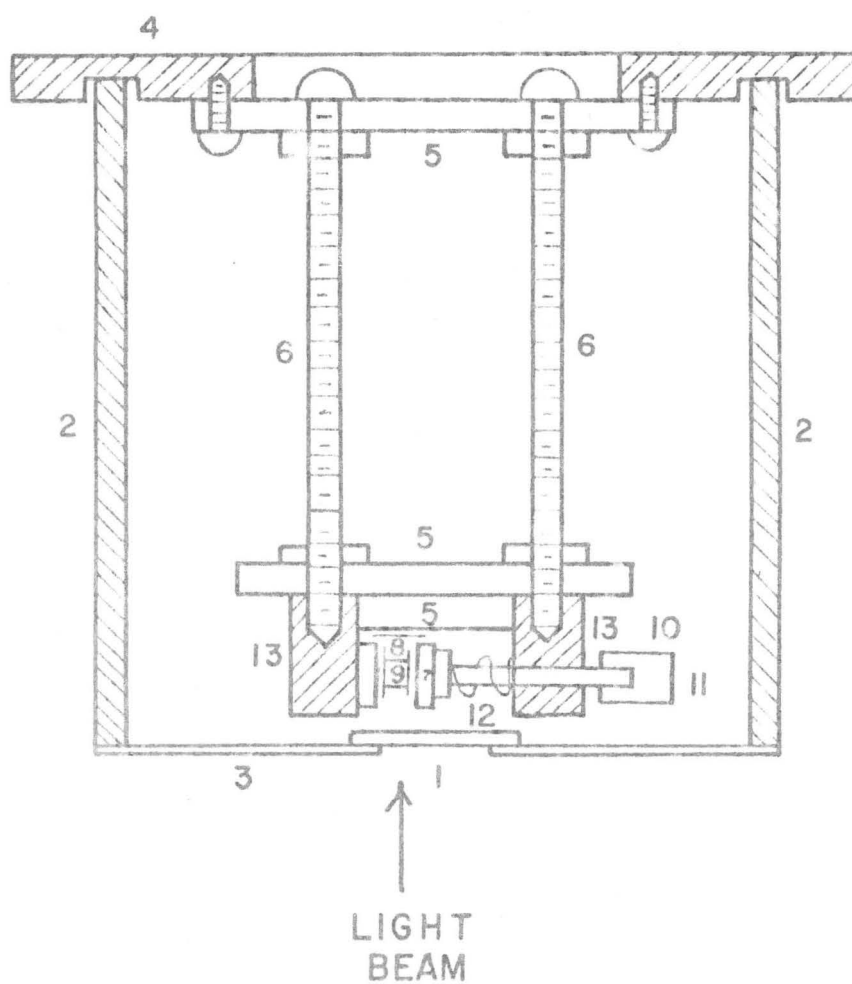
Recalling equation (2) and the estimated maximum value of N_e given on page 75, the concentration of holes is seen to be approximately equal to the concentration

of temporarily trapped electrons, N_e' . In the case of photoconduction in the F-band, the "holes" are negative ion vacancies. Hence, 10^{15} cm^{-3} can also be considered to be the lower limit of N_h^0 in the equations given in Part IV. A higher value for N_h^0 may apply to certain crystals where a higher excitation rate, F , is employed, or where the initial concentration of halide ion vacancies is higher than 10^{15} cm^{-3} in the virgin crystal.

It is believed that the greater bleaching rate observed at very low exposures in most of the curves reported in graphs 8 and 9, is another manifestation of the presence of these thermally unstable trapping centers. At the start of an illumination period these traps readily absorb photoelectrons while few are being thermally released. Hence, the bleaching rate of F-centers would be expected to be higher in this exposure region because of the very low electron-vacancy recombination rate. Since equation (11) was based on the assumption that an equilibrium photoelectron concentration had been achieved, only the upper linear portions of the bleaching curves were used for the theoretical treatment contained in the previous section. The bend in the bleaching curves generally occurred after a 2-minute exposure, which corresponds closely to the time for attainment of equilibrium as revealed by graph 4.

PLATE I

PHOTOCONDUCTIVITY CELL



LEGEND

1. glass window
2. brass cylinder, 5 x 5 cm.
3. sheet-metal lid
4. brass base plate, 7 cm. square
5. "Teflon" insulating plates
6. brass bolts
7. carbon electrodes, 6 x 10 mm.
8. solid aluminum mirrors, 4 x 10 mm.
9. KCl sample
10. spring-loaded rod
11. rubber handle
12. spring
13. brass mounting blocks

PLATE 2

SIMPLIFIED CIRCUIT DIAGRAM OF AMPLIFIER

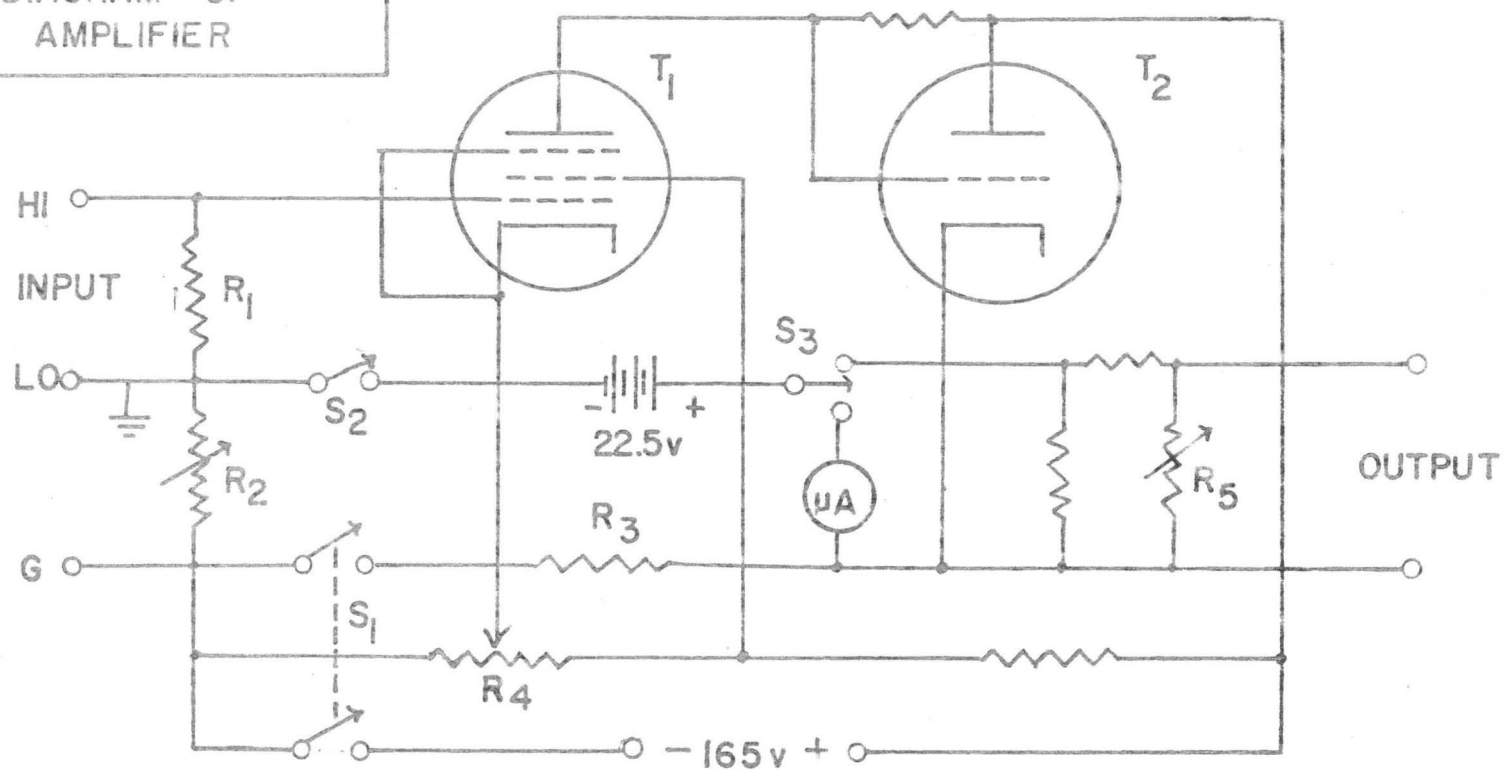
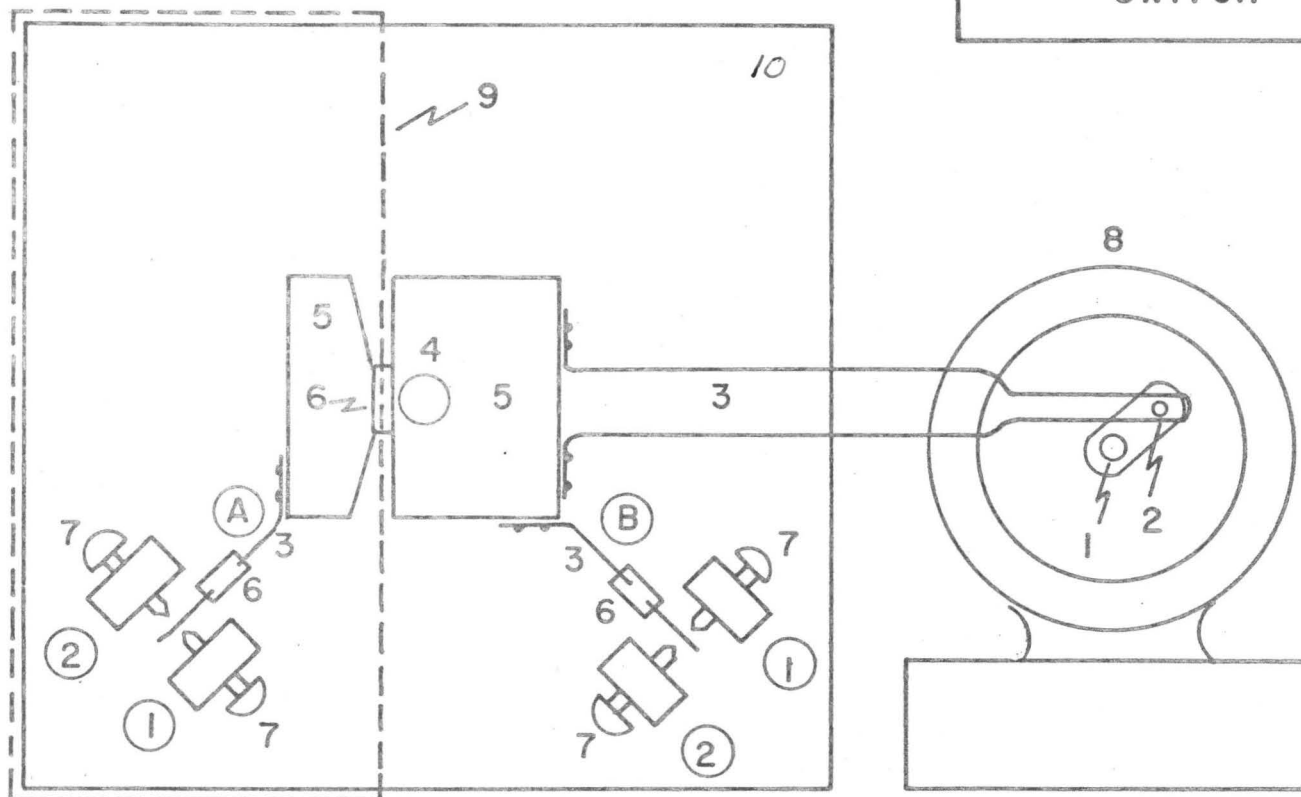


PLATE 3

MOTOR - DRIVEN SWITCH



LEGEND

1. motor shaft
2. eccentric cam
3. spring-metal strips
4. bearing
5. one-quarter inch plywood
6. "Teflon" insulation
7. adjustable terminals
(brass screws)
8. 6-12 volt D.C. motor
9. sheet-metal shielding
10. plywood mounting board, 13 cm. square

SEQUENCE OF OPERATION

B₂ closes

A₁ opens

A₂ closes

A₁ closes

B₂ opens

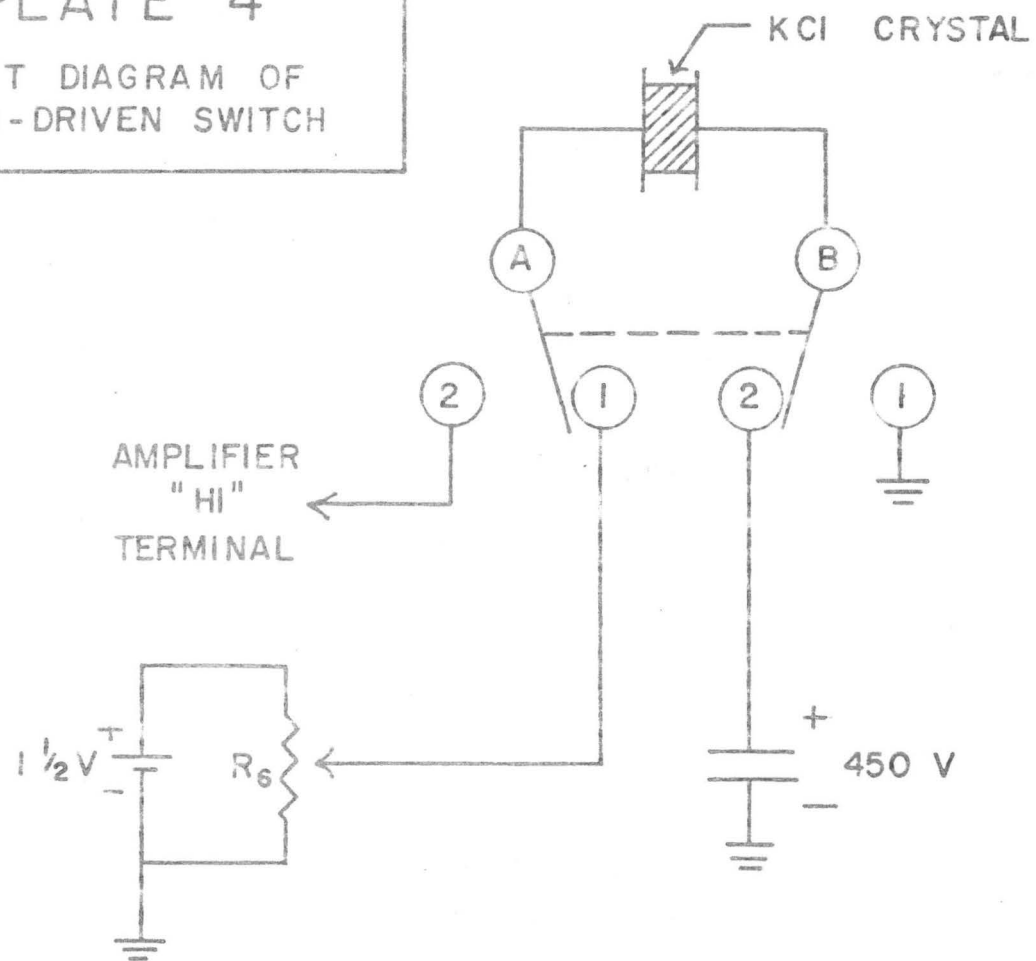
B₁ closes

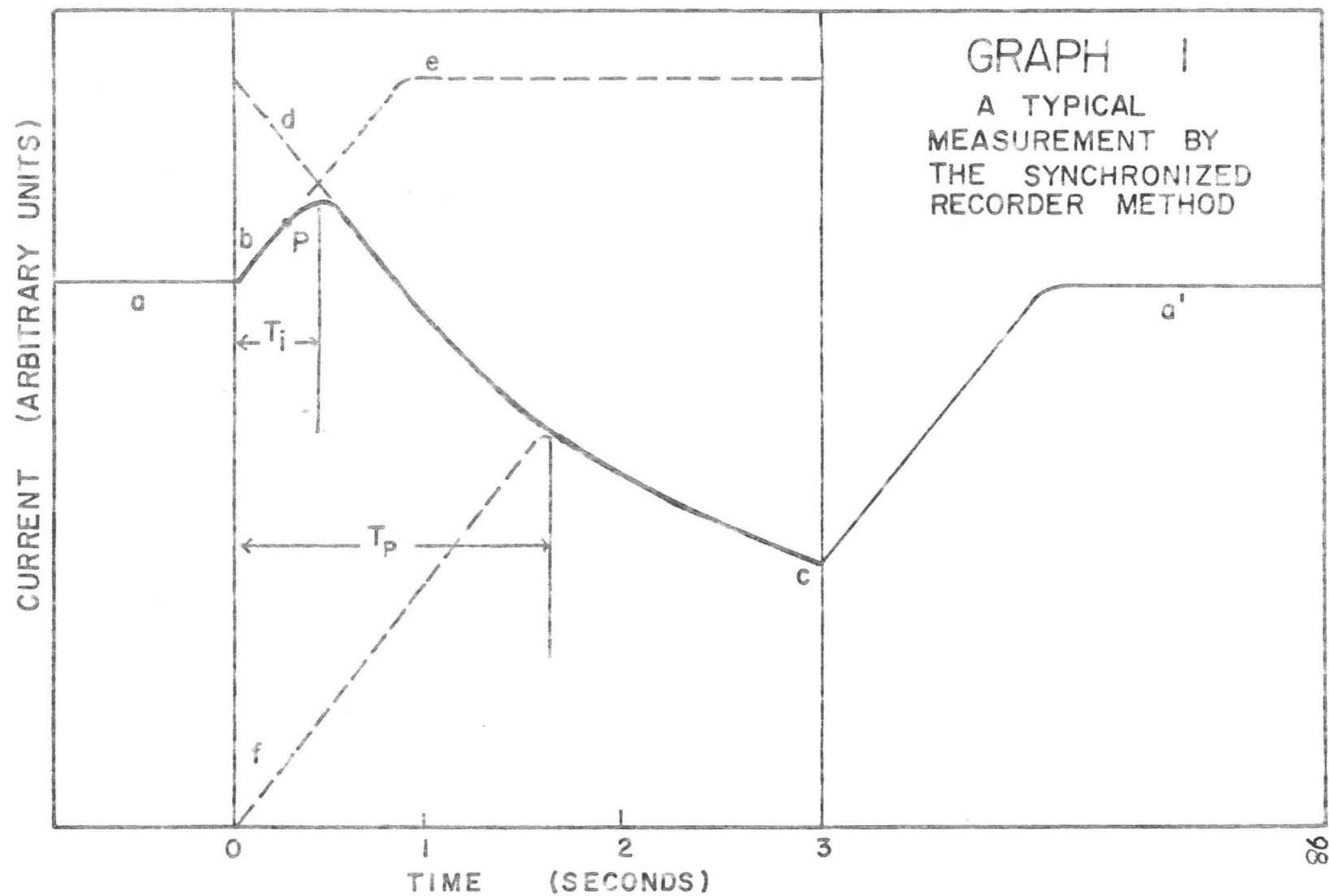
B₁ opens

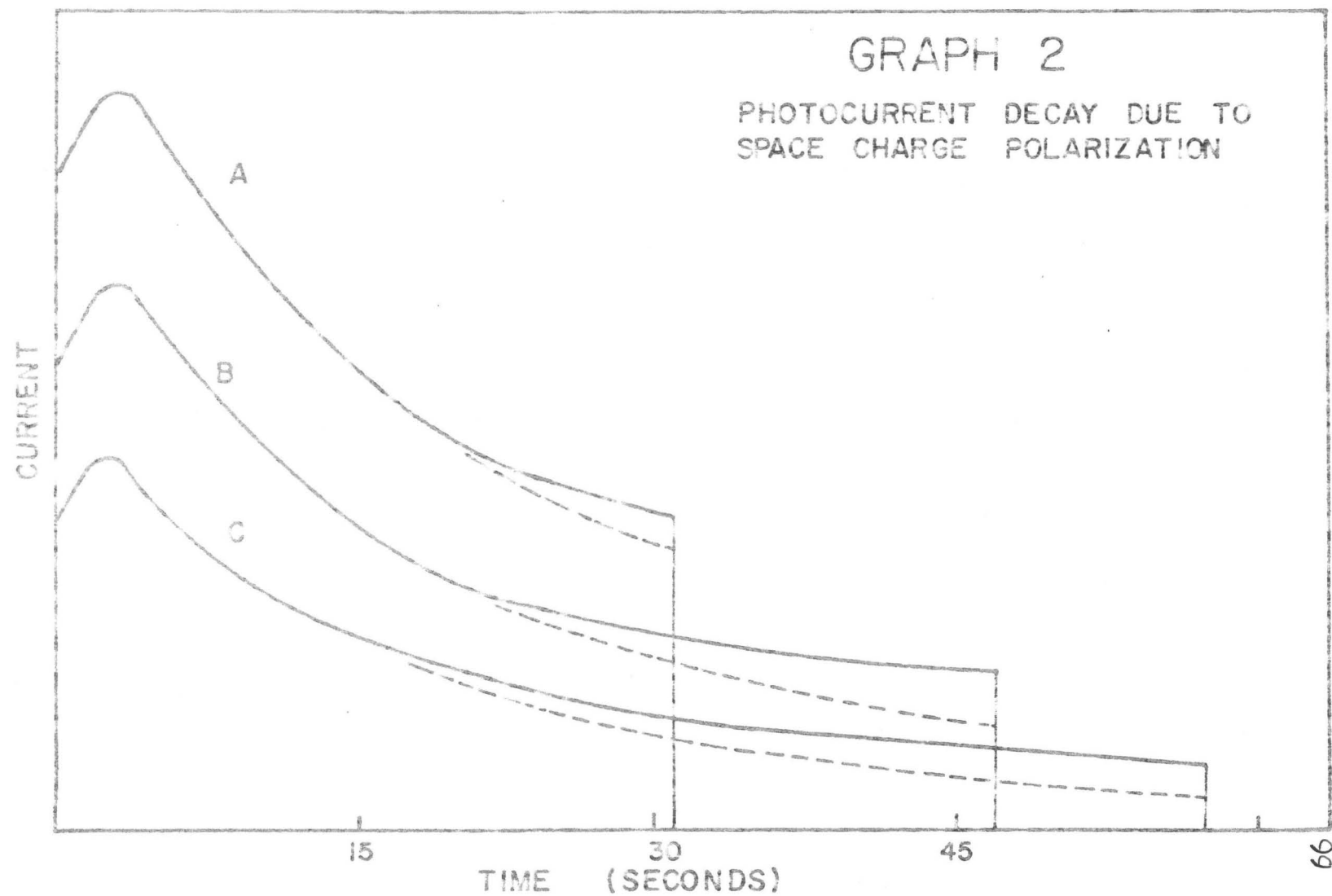
B₂ closes

PLATE 4

CIRCUIT DIAGRAM OF
MOTOR-DRIVEN SWITCH

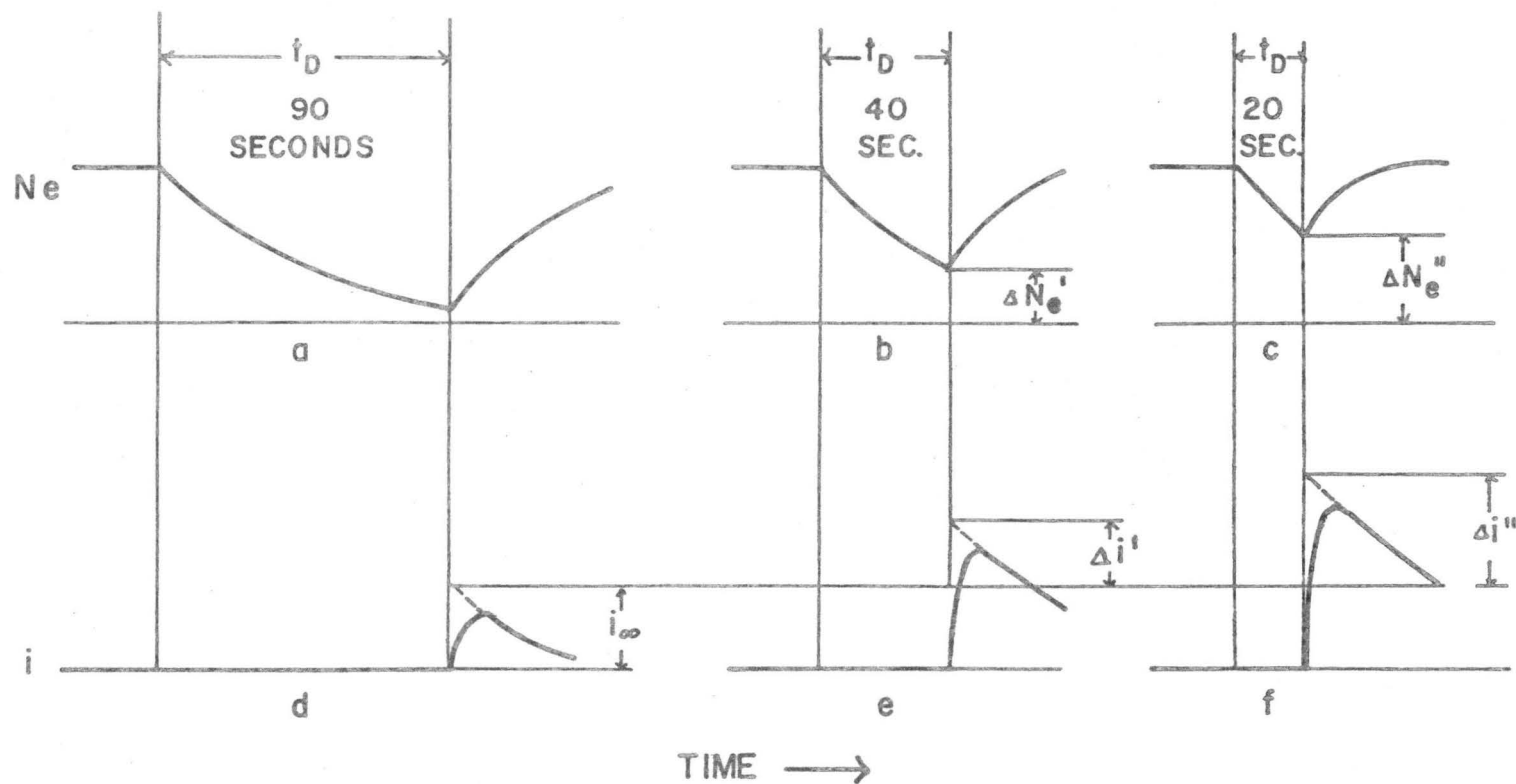




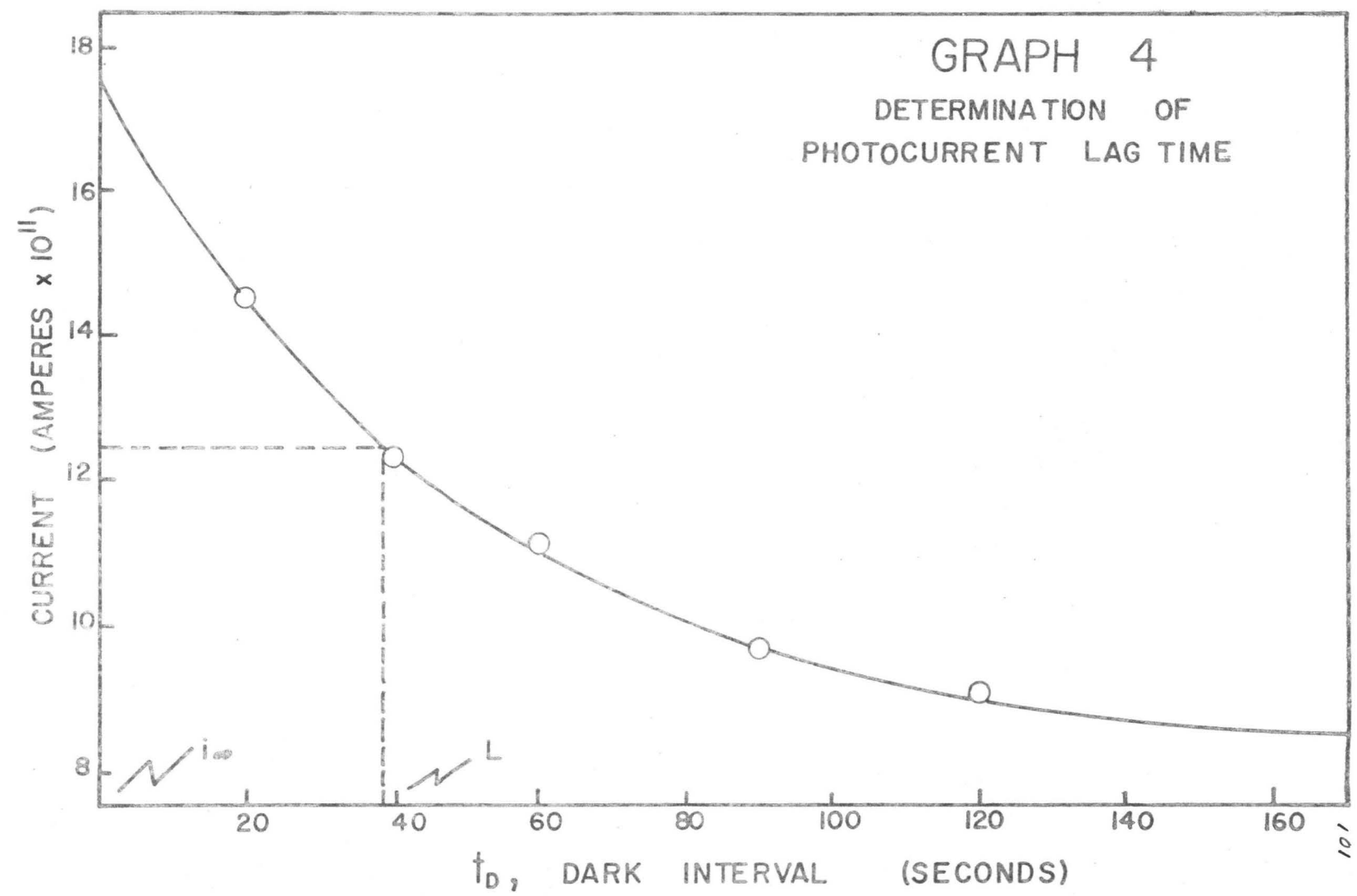


GRAPH 3

EXPERIMENTAL METHOD FOR DETERMINING PHOTOCURRENT LAG TIME

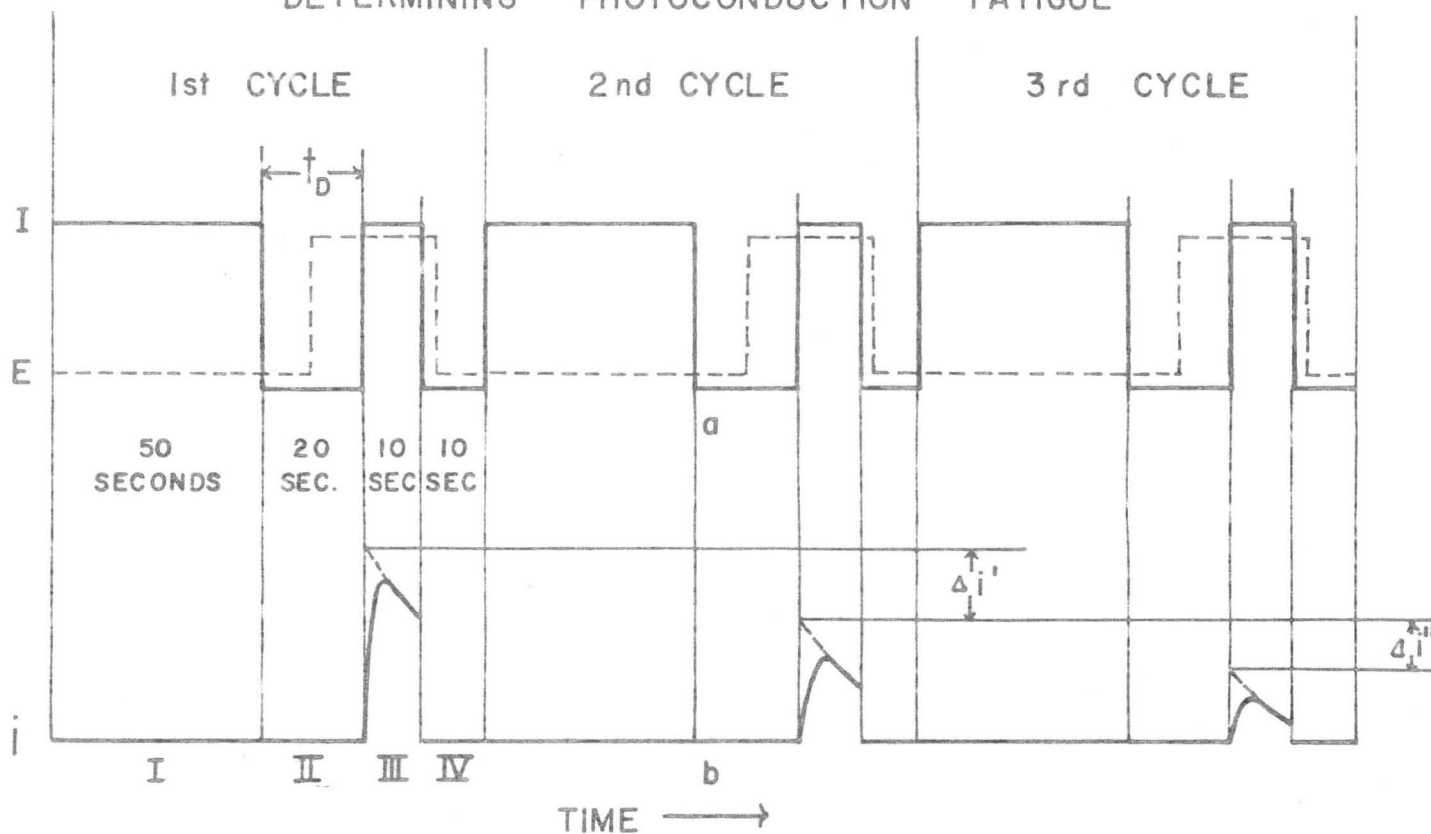


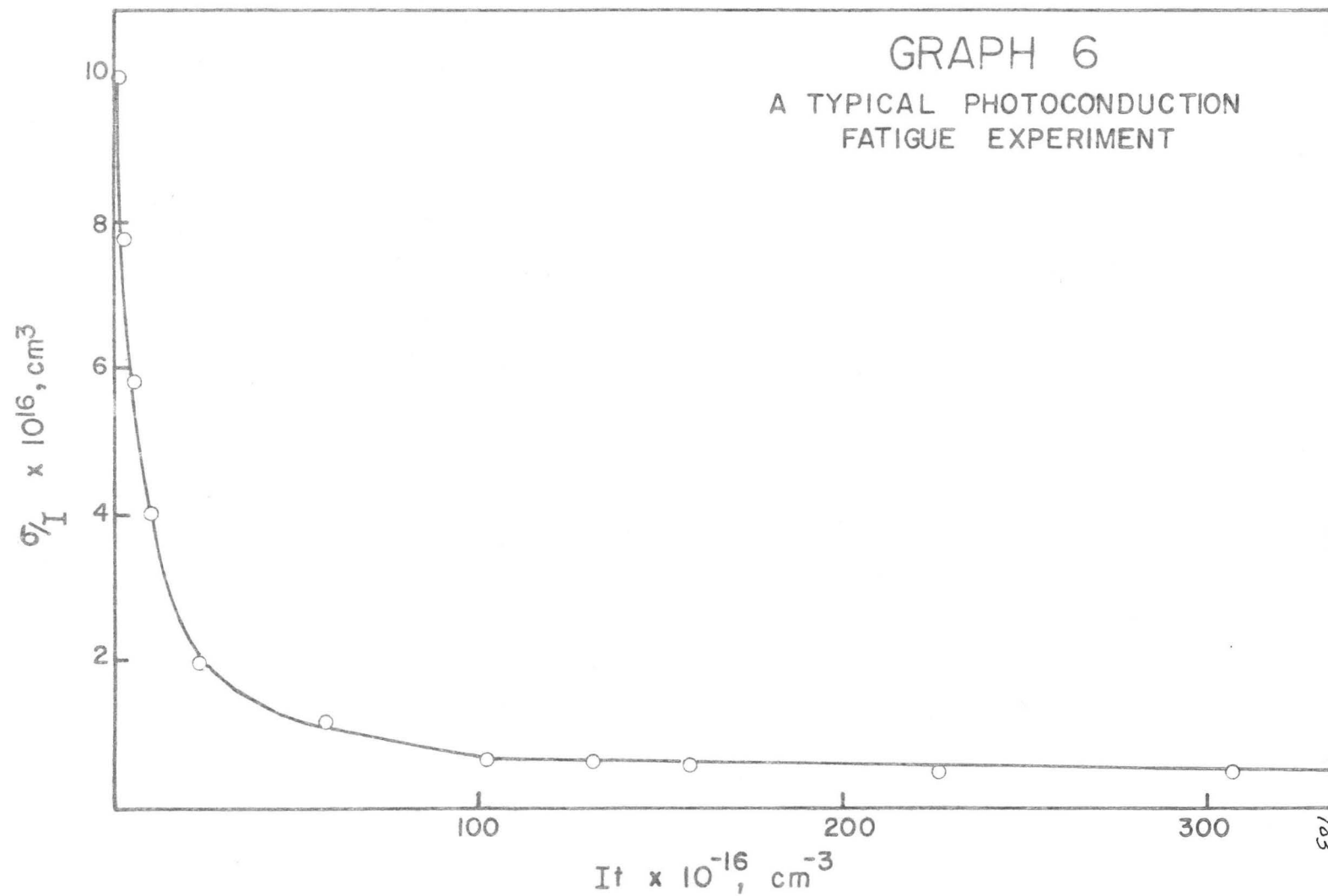
GRAPH 4
DETERMINATION OF
PHOTOCURRENT LAG TIME

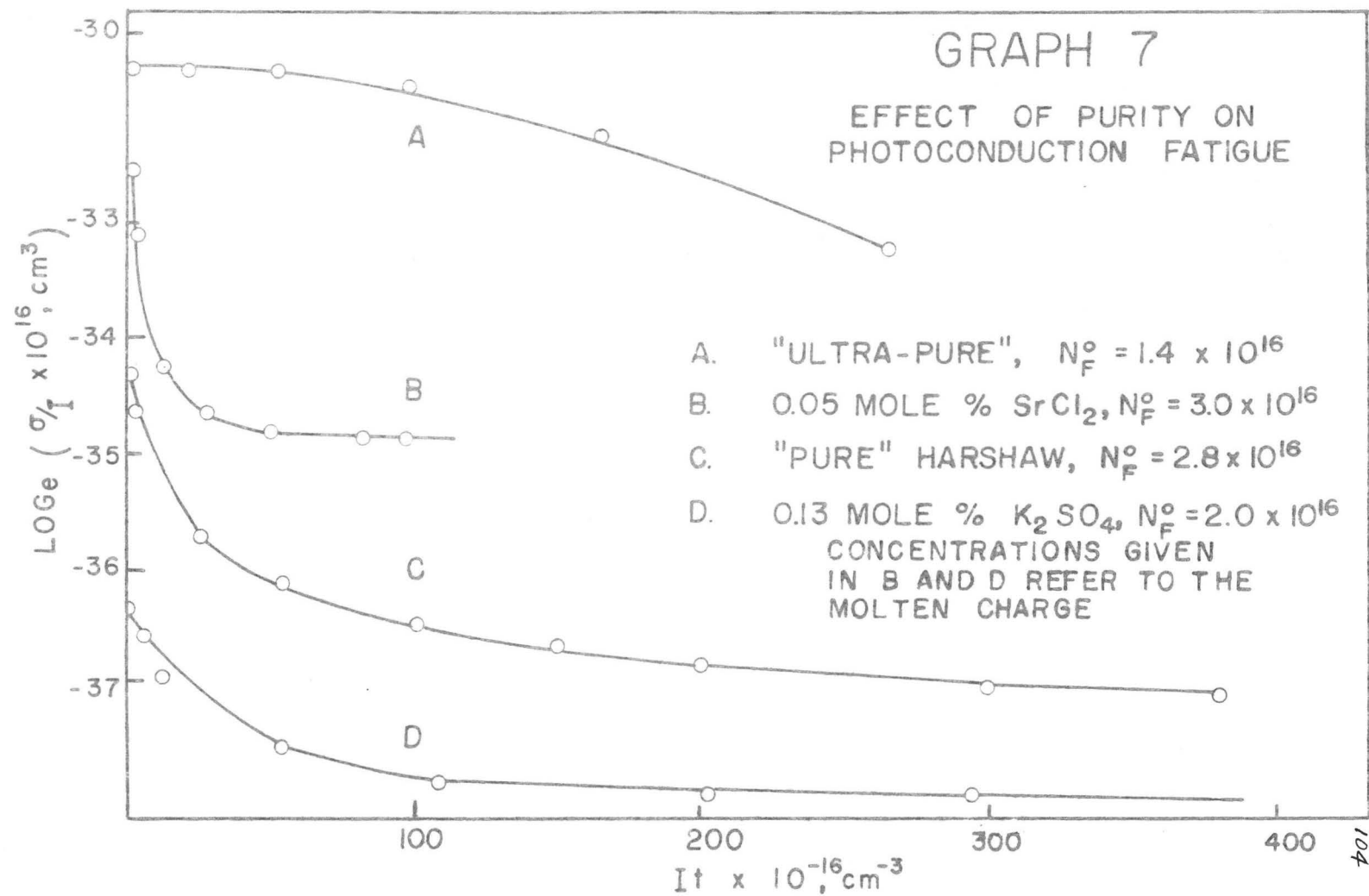


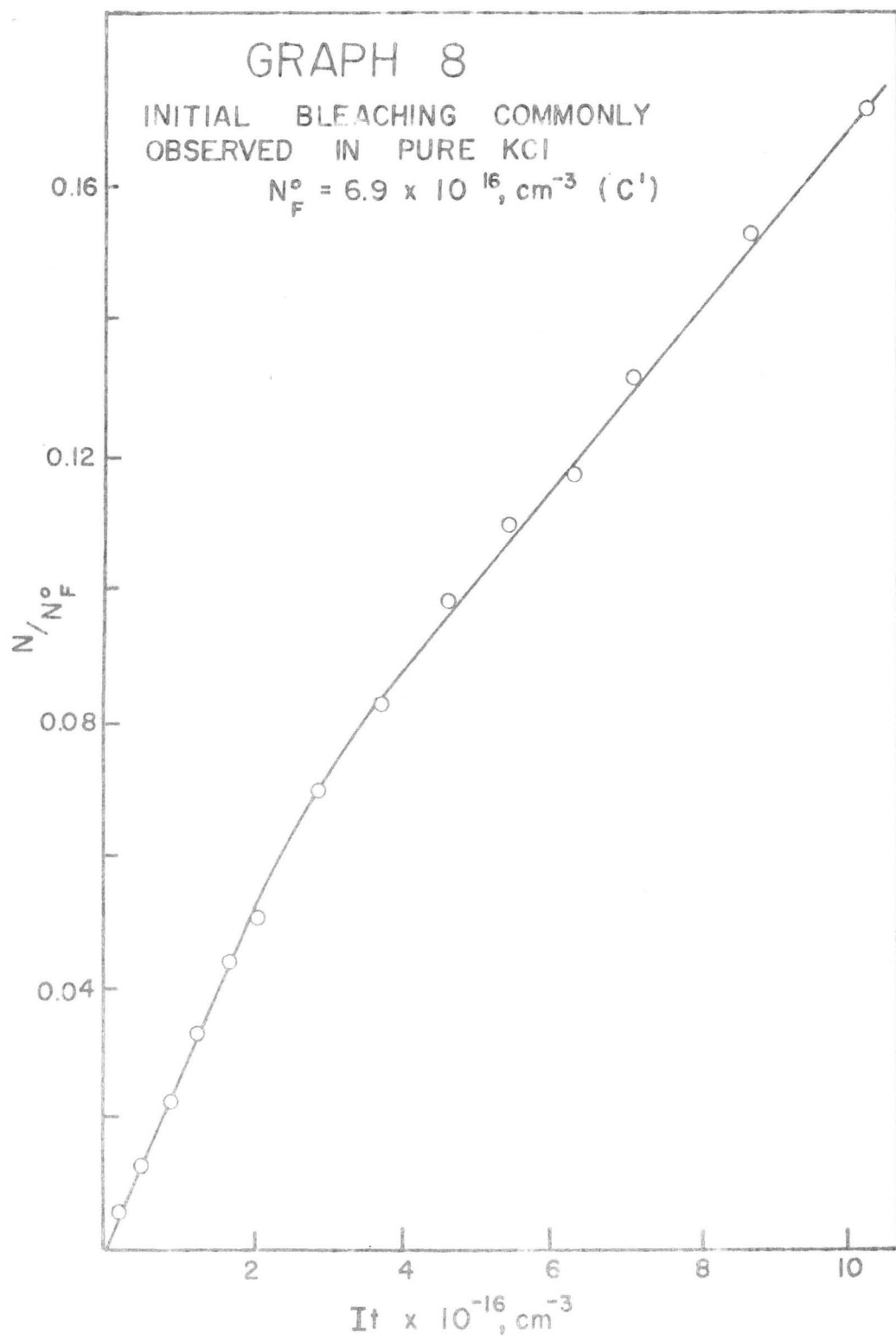
GRAPH 5

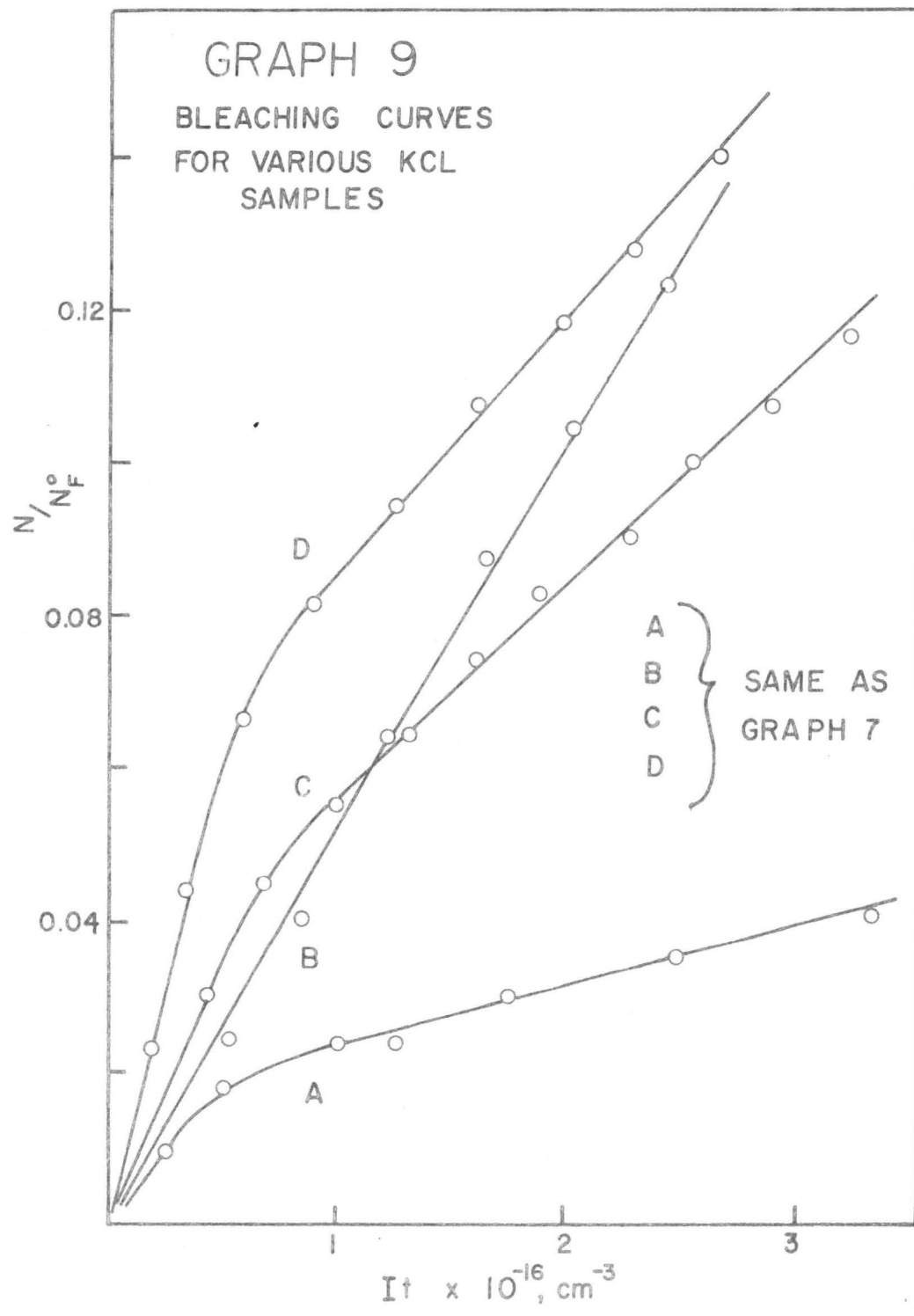
EXPERIMENTAL METHOD FOR
DETERMINING PHOTOCONDUCTION FATIGUE

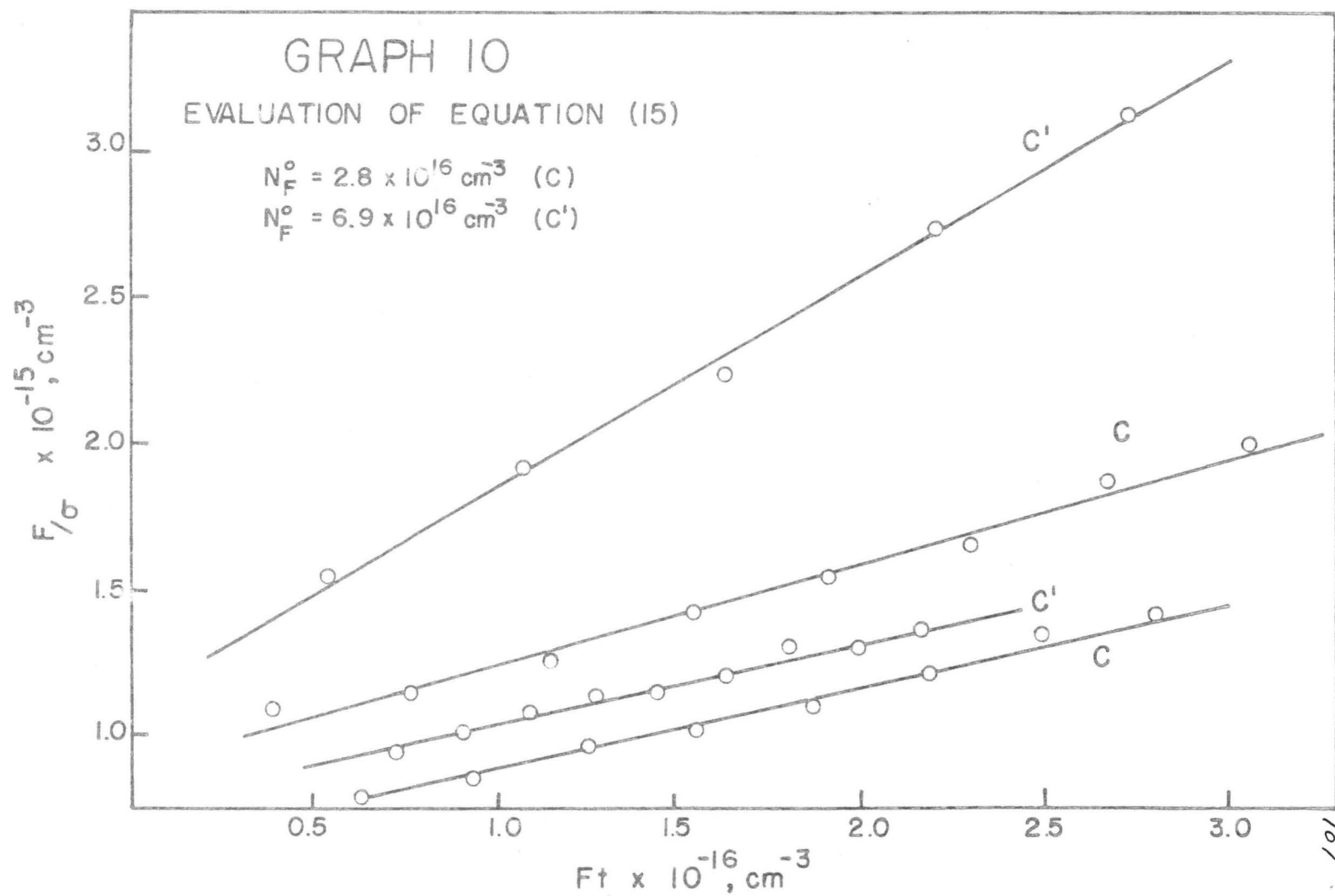


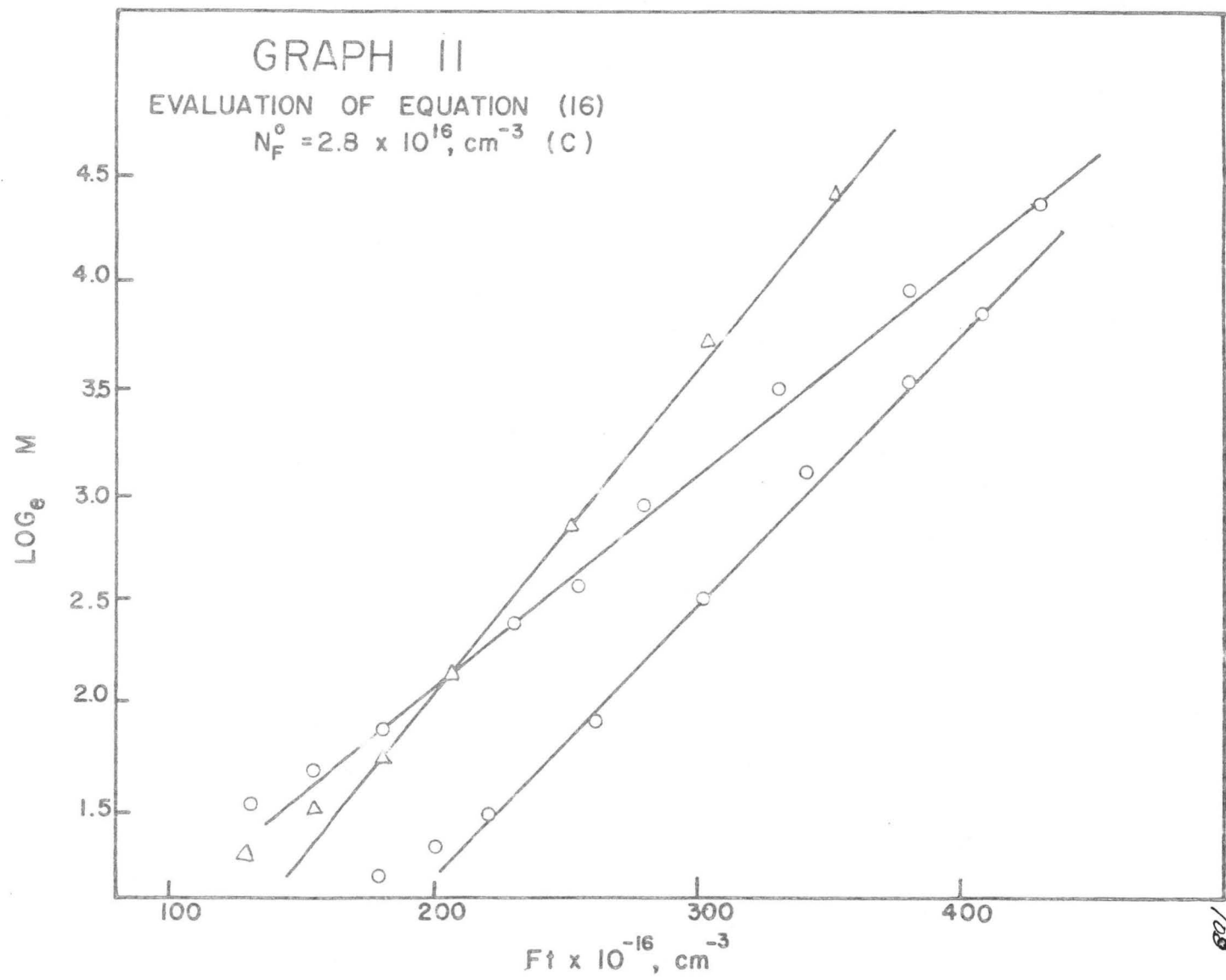












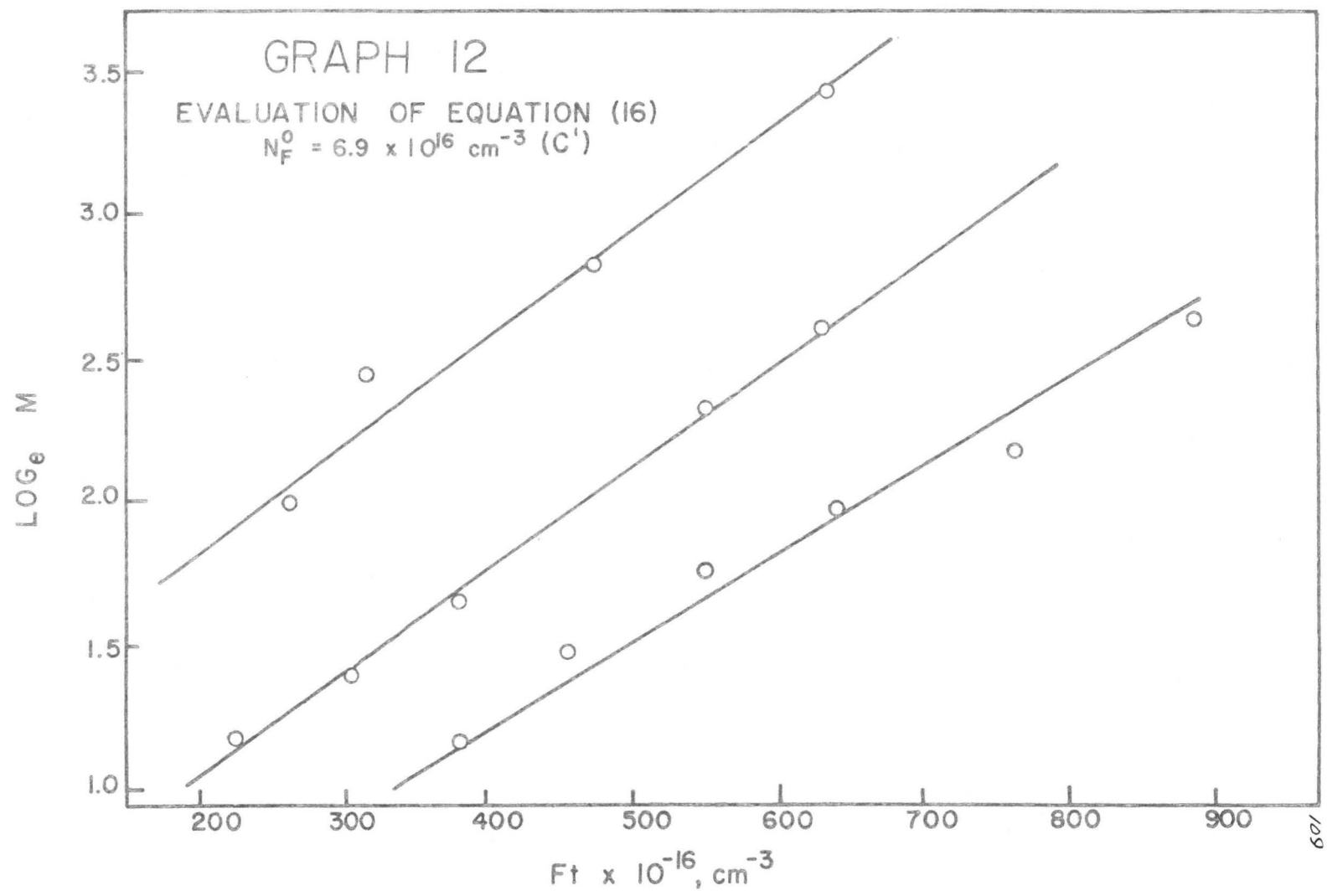


TABLE 1

Theoretical and Experimental Polarization Field
Strengths after Various Charge Passages

Charge Passed (coulombs)	Theoretical E (volt/m)	Observed Ep (volt/m)	% of Applied Field Strength	Appearance in Graph 2
0.9×10^{-10}	1.3×10^5	1.0×10^5	49	curve A
1.7	2.1	1.2	65	" B
2.9	2.8	1.6	69	not shown
3.5	3.0	1.7	72	curve C

TABLE 2

Polarization Field Strengths after
Various Charge Passages using Motor-Driven Switch
with an Applied Field of 370 volts/mm

Charge Passed (coulombs)	Observed Ep (volt/mm)
0.1×10^{-9}	115
0.4	125
1.8	130
2.4	125
4.5	128
9.0	125

TABLE 3

The Effect of Aging on Photoresponse
Before and After Fatigue; $N_F^0 = 6.9 \times 10^{16} \text{ cm}^{-3}$

Time after Furnace Removal	δ/I Before Fatigue	δ/I After Fatigue
1.3 hours	$1.1 \times 10^{-15} \text{ cm}^3$	$3.6 \times 10^{-17} \text{ cm}^3$
5 days	0.9	4.3
10 days	0.7	6.4
7 weeks	1.0	6.3

TABLE 4

The Effect of Aging on Photoresponse
Before and After Fatigue; $N_F^0 = 2.8 \times 10^{16} \text{ cm}^{-3}$

Time after Furnace Removal	δ/I Before Fatigue	δ/I After Fatigue
0.5 hour	$0.9 \times 10^{-15} \text{ cm}^3$	$6.0 \times 10^{-17} \text{ cm}^3$
1 day	1.4	7.0
2 weeks	0.8	7.3

TABLE 5

Comparison of Multiple F-center Theory
with Experimentally Determined Bleaching Rates

Source	Observed Rate (Slope)	Rate from Equation (A7)	Rate from Equation (A8)
Graph 8	0.090	0.30	0.38
Graph 9, line B	0.150	0.29	0.37
" 9, " C	0.077	0.34	0.40
" 9, " D	0.067	0.40	0.44

TABLE 6

Estimated Trap Concentrations and Cross Sections

Code Letter From Graphs 9-12	S_h (cm^2)	N_h^0 (cm^{-3})	S_t (cm^2)	N_t^0 (cm^{-3})
B	4.1×10^{-12}	2.4×10^{15}	1.7×10^{-13}	0.9×10^{16}
C	3.0×10^{-13}	1.7	3.9×10^{-15}	1.0
C'	3.6×10^{-13}	1.7	2.8×10^{-15}	2.1
D	9.2×10^{-14}	2.2	1.7×10^{-15}	0.8

BIBLIOGRAPHY

1. Burstein, E. and J. J. Oberly. Photoconductivity of trapped electrons in the alkali halides. The Physical Review 79:217. 1950.
2. Duerig, William H. and Jordan J. Markham. Color centers in alkali halides at 5° K. The Physical Review 88:1043-1049. 1952.
3. Flechsig, Werner. "Über die Sättigung des lichtelektrischen Primärstromes in Kristallen. Zeitschrift für Physik 46:788-797. 1928.
4. Forsythe, W. E. Measurement of radiant energy. New York, McGraw-Hill, 1937. 452 p.
5. Gyulai, Z. Lichtelektrische und optische Messungen an blauen und gelben Steinsalz-Kristallen. Zeitschrift für Physik 35:411-420. 1926.
6. Harrison, George R. MIT wavelength tables. New York, J. Wiley & Sons, 1939. 429 p.
7. Hogness, T. R., F. P. Zscheile, Jr., and A. E. Sidwell, Jr. Photoelectric spectrophotometry. The Journal of Physical Chemistry 41:379-415. 1937.
8. Hughes, Arthur Llewelyn and Lee Alvin DuBridge. Photoelectric phenomena. New York, McGraw-Hill, 1932. 531 p.
9. Inchauspé, Nicolas. Photoconduction in KBr and KI containing F centers. The Physical Review 106: 898-903. 1957.
10. Konitzer, John D. and Jordan J. Markham. Effect of bleaching on the optical band width of the F center in KCl. The Physical Review 107:685-686. 1957.
11. Launer, Herbert F. An easily constructed, rugged, sensitive thermopile. The Review of Scientific Instruments 11:98-101. 1940.
12. MacDonald, J. Ross. Capacitance and conductance effects in photoconducting alkali halide crystals. The Journal of Chemical Physics 23:275-295. 1955.

13. MacDonald, J. Ross. Photocontrolled low frequency dielectric dispersion. The Physical Review 85: 381. 1952.
14. Markham, Jordan J. et al. Bleaching properties of F centers in KBr at 5° K. The Physical Review 92:597-603. 1954.
15. Markham, Jordan J. The interaction of color centers with their environment. The Journal of Physical Chemistry 57:762-771. 1953.
16. Markham, Jordan J. Soft and hard F-centers. The Physical Review 86:433. 1952.
17. Mott, N. F. and R. W. Gurney. Electronic processes in ionic crystals. 2nd ed. Oxford, Oxford University Press, 1950. 275 p.
18. Neilson, George W. and Allen B. Scott. Photoconductance of F-centers and their aggregates. In: Report of the conference on defects in crystalline solids held at the H. H. Wills Physical Laboratory, University of Bristol, July 1954, London, The Physical Society, 1955. p. 297-303.
19. Oberly, J. J. Photoconductivity of trapped electrons in KBr crystals at room temperature. The Physical Review 84:1257-1258. 1951.
20. Petritz, Richard L. The relation between lifetime, limit of sensitivity, and information rate in photoconductors. In: Photoconductivity conference held at Atlantic City, Nov. 1954, New York, John Wiley & Sons, 1956. p. 49-77.
21. Petroff, St. Photochemische Beobachtungen an KCl-Kristallen. Zeitschrift für Physik 127:443-454. 1950.
22. Pick, H. Über den Einfluss der Temperatur auf die Erregung von Farbzentren. Annalen der Physik 31: 365-376. 1938.
23. Pohl, R. W. Electron conductivity and photochemical processes in alkali-halide crystals. Proceedings of the Physical Society 49 (extra part):3-30. 1937.

24. Przibram, Karl. Verförbung und Lumineszenz durch Becquerelstrahlen. III. Zeitschrift für Physik 68:403-422. 1931.
25. Redfield, Alfred G. Electronic Hall effect in the alkali halides. The Physical Review 94:537-540. 1954.
26. Roberts, Shepard. A feedback micromicroammeter. Review of Scientific Instruments 10:181-183. 1939.
27. Röntgen, W. C. Über die Elektrizitätsleitung in einigen Kristallen und über den Einfluss einer Bestrahlung darauf. Annalen der Physik 64:1-195. 1921.
28. Rose, Albert. An outline of some photoconductive processes. RCA Review 12:362-414. 1951.
29. Rose, Albert. Performance of photoconductors. Proceedings of the Institute of Radio Engineers 43:1850-1869. 1955.
30. Rose, Albert. Recombination processes in insulators and semiconductors. The Physical Review 97:322-333. 1955.
31. Scott, Allen B. and Lamar P. Bupp. The equilibrium between F-centers and higher aggregates in KCl. The Physical Review 79:341-346. 1950.
32. Seitz, Frederick. Color centers in alkali halide crystals. Reviews of Modern Physics 18:384-408. 1946.
33. Seitz, Frederick. Color centers in alk. halide crystals. II. Reviews of Modern Physics 26:7-94. 1954.
34. Simpson, J. H. Charge distribution and energy levels of trapped electrons in ionic solids. Proceedings of the Royal Society of London, ser. A, Mathematical and Physical Sciences 197:269-281. 1949.
35. Tibbs, S. R. Electron energy levels in NaCl. Transactions of the Faraday Society 35:1471-1484. 1939.

36. Ueta, Masayasu and Werner Känzig. Generation of electron traps by plastic flow in alkali halides. The Physical Review 97:1591-1595. 1955.
37. van Doorn, C. Z. and Y. Haven. Dichroism of the F and M absorption bands in KCl. The Physical Review 100:753. 1955.
38. von Hippel, A. et al. Photocurrent, space-charge buildup, and field emission in alkali halide crystals. The Physical Review 91:568-579. 1953.